Object-based machine learning correction of LiDAR using RTK-GNSS to model the potential effects of sea-level rise in Swanquarter National Wildlife Refuge, North Carolina

by

Michelle R. Schlup

May 2020

Director of Thesis: Hannah M. Cooper

Major Department: Geography, Planning and Environment

Coastal wetland systems are a vital habitat that provide many beneficial services; however, the complexity of these habitats makes it difficult for conservation managers to preserve these environments and predict future changes. Sea-level rise (SLR) is a growing and accelerating threat to coastal wetlands making its predictability essential for conservation planners. Light Detection and Ranging (LiDAR) Digital Elevation Models (DEMs) have become an important component in monitoring coastal wildlife refuges and are implemented into models like Sea Level Affecting Marshes Model (SLAMM) to produce SLR vulnerability assessments. Although, with dense vegetation in these environments LiDAR penetration is reduced and DEMs in turn are less accurate. This study implemented an Object-Based Machine Learning (OBML) technique to improve DEM accuracy at Swanquarter National Wildlife Refuge (SNWR) and was implemented into SLAMM to provide land cover maps of the year 2050 for land cover change analysis. The corrected OBML DEM was compared with the original LiDAR DEM obtained from North Carolina Floodplain Mapping Program (NCFMP), which found the OBML DEM to provide a more reliable depiction of the potential impacts of future SLR on the coastal wetlands in North Carolina. Conservation managers may find the OBML approach in this study to be a useful option for SLR analysis.

Object-based machine learning correction of LiDAR using RTK-GNSS to model the potential effects of sea-level rise in Swanquarter National Wildlife Refuge, North Carolina

A Thesis

Presented To the Faculty of the Department of Geography, Planning and Environment

East Carolina University

In Partial Fulfillment of the Requirements for the Degree

Master of Science in Geography

by

Michelle Schlup

May 2020

Object-based machine learning correction of LiDAR using RTK-GNSS to model the potential effects of sea-level rise in Swanquarter National Wildlife Refuge, North Carolina

by

Michelle Schlup

APPROVED BY:

DIRECTOR OF

THESIS: _____

(Hannah Cooper, PhD)

COMMITTEE MEMBER: _____

(Paul Gares, PhD)

COMMITTEE MEMBER: _____

(Thad Wasklewicz, PhD)

CHAIR OF THE DEPARTMENT

OF GEOGRAPHY, PLANNING AND ENVIRONMENT: _____

(Thad Wasklewicz, PhD)

DEAN OF THE

GRADUATE SCHOOL: _____

(Paul J. Gemperline, PhD)

DEDICATIONS

I would like to dedicate my thesis to my family who have helped give me the opportunity to obtain an advanced degree that has provided me with invaluable skills to help me succeed throughout my life. They have continually provided me with support and motivation to reach my goals and I could not thank them enough for all they have done for me.

ACKNOWLEDGMENTS

This research was made possible by my advisor (Hannah Cooper) and committee members (Paul Gares, Thad Wasklewicz) who are part of the Geography, Planning, and Environment Department at East Carolina University.

I would also like to thank the help given from the staff at Lake Mattamuskeet National Wildlife Refuge who oversee Swanquarter National Wildlife Refuge.

TABLE OF CONTENTS

LIST OF TABLES

LIST OF FIGURES

1. Introduction

1.1 Wetland Systems and their Importance

There are many types of wetlands along the eastern coast of North America that provide habitat for numerous kinds of vegetation and wildlife. Examples of wetland types include tidal salt, brackish marsh, mangrove, freshwater marsh, wooded/shrub wetland, and many more, each occurring at varying elevations. Low and high marshes are found at different elevations so different inundation rates and vegetation species occur there. A low marsh has an elevation closer to sea-level, while the high marsh has a higher elevation, so the low marsh floods more frequently than the high marsh. Low marsh tends to be located along the coast, creeks, canals, and ditches, while the high marsh is more wide-ranging and is positioned between the low marsh and the upland edge. Vegetation in the low marsh can tolerate higher levels of inundation than the vegetation in the high marsh (NHDES, 2004). Wetlands are a vital habitat for countless species of terrestrial and aquatic vegetation and wildlife. Ecotones, which is the transitional zone between aquatic and terrestrial biomes, provide many ecosystem services; for example, they recharge aquifers, filter run-off and create a buffer protecting the coast from storm damage (Turpie et al., 2015). Other benefits to coastal habitats include nutrient coastal defense, shoreline protection, and reduction in nutrient intensification (Cadol et al., 2016). Wetlands are as important to humans as they are to the species that live in them, but they are very multifaceted.

Between upland and mudflat areas are intertidal marshes, which generate zones of vegetation through biogeomorphic feedbacks. Wetland systems are very complex with many interrelated parts, so one change in the system can cause a major shift in another part of the system or could change the entire system all together. Patterns can be seen in different wetland components. A study by Moffett & Gorelick (2016), using differing marsh ages and types of

marshes, found that marsh salinity and vegetation pattern complexity correlate significantly, but the elevation and age of the marsh were found to be independent. Channel complexity also correlated with vegetation age and pattern complexity. Even though marshes may share a physical environment, the ecosystem composition can be completely different; marsh age does not automatically equal a more or less complex system; salt marshes can maintain a stable system even with the correlation of two complex elements, channels and vegetation (Moffett & Gorelick, 2016). It is difficult to understand the structure of a wetland because of the complex feedbacks that occur in these environments causing a wetland's adaptability from natural and artificial alterations to be in question.

Wetland ecosystems are one of the most threatened environments, and the majority of salt marshes in the USA have been damaged from human activity (Neckles et al., 2015). Coastal wetlands have experienced both artificial and natural modifications worldwide (i.e. dredging and filling, fragmentation, hydrological changes, impoundments, pollution, rising sea levels) causing stress to these systems (Turpie et al., 2015). Monitoring and adaptation planning should be conducted to protect and restore wetlands. Although, restoration efforts have become a challenge for coastal managers since coastal wetlands are a very complex and dynamic environmental system (Neckles et al., 2015). It is difficult to make predictions of their changes with the uncertainty of the future environment and biogeomorphic feedbacks. This is notably a problem with the changing of the climate and the accelerated increase in sea levels.

1.2 Wetlands and Sea-Level Rise (SLR)

Global warming has led to sea-level rise (SLR) from melting glaciers and thermal expansion of the oceans. The Intergovernmental Panel on Climate Change (IPCC) continually reports on the rate of SLR and projects that the rate of SLR will increase throughout this century

(NOAA et al., 2017). Coastal landscapes are predicted to submerge underwater at different levels and respond either statically (inundation) or dynamically (landform/landscape change) (Lentz et al., 2015). Wetlands will have to migrate at the same rate as the rising sea-level to survive, as well as have available area to migrate into, which can become a problem in developed spaces (Linhoss et al., 2015). Climate change has caused increasing SLR as well as an increased frequency and intensity of hurricanes and storm surges causing coastal areas to increase in inundation (Maloney & Preston, 2014). Marsh migration, SLR, and storm surges have shown to be contingent on elements such as local topography, storm intensity and the storm's path. There are over 150 coastal National Wildlife Refuges in the United States home to many different vegetation and wildlife species and with increasing SLR wetlands can be restructured, habitats types can shift and migrate inland, and inundation can occur (Liu & Delach, 2015).

However, wetlands have many mechanisms that make them resilient, but it is uncertain depending on the rate of SLR. Wetlands are influenced greatly by vertical land movement (VLM). VLM rates vary worldwide due to the phenomenon called isostacy, which is the rising and falling of the Earth's crust. The eastern coast of the United States is experiencing a higher rate of SLR on average because of regional subsidence that is occurring there putting the east coast at a higher risk (Beckett et al., 2016). Tidal marshes are able to sustain their elevation in relation to the sea, though, from the dynamic feedback system of sediment accretion (Schile et al., 2014). Sediment and biomass accretion allow wetlands to gain vertical growth, which helps wetlands resist against SLR. Coastal wetlands vary in sediment dynamics and vegetation structure, productivity, and decomposition which may cause wetlands to respond differently to SLR (Beckett et al., 2016).

Wetland resiliency is also based upon a biogeomorphic and hydrodynamic relationship. There are feedbacks between vegetation and flooding in a wetland that helps it stabilize against SLR, but stabilization may become an issue with accelerated SLR (Morris et al., 2013). Wetland vegetation species are highly impacted by flow attenuation, which modifies the wet-dry regime and inundation depth and is very particular for each species of vegetation. This causes vegetation species to become more susceptible to SLR (Rodríguez et al., 2017). Another, important hydrological element to vegetation is the hydroperiod. A hydroperiod, or period of flooding, is established by marsh surface elevation and its relation to mean high water. A hydroperiod greatly influences the plant growth in a wetland, because vegetation exists only at certain elevations based upon its hydrological tolerance (Morris et al., 2013).

Although wetlands are very resilient, these systems should be monitored, because there are uncertainties on how well coastal wetlands will respond to increased SLR, sediment reduction, vegetation productivity reduction from inundation increases, and restricted marsh migration habitat (Schile et al., 2014; Cadol et al., 2016). Each wetland type responds differently to SLR making them very difficult to monitor and protect (Linhoss et al., 2015; Tabak et al., 2016; Bigalbal et al., 2018). The changing of the climate, SLR, and landcover change have been shown to endanger biodiversity, and low-lying coastal areas are one of the most vulnerable regions to the impacts of SLR (Reece & Noss, 2014). SLR is predicted to cause habitat change and loss that impacts coastal species, and many studies have been conducted to preserve wetland habitats to protect the species in them, such as shorebird populations. Changes in habitat and habitat availability caused by SLR may cause the distribution and abundance of wetland bird species to become altered (Iwamura et al., 2013; Veloz et al., 2013). Impacts from SLR for the

future is very uncertain for wetland environments, which causes restoration efforts to be very intricate, difficult challenges (Veloz et al., 2013).

1.3 Significance of Digital Elevation Models (DEMs) of coastal National Wildlife Refuges

While sediment, hydrology, and vegetation factors are all important, the spatial variability of elevation is one that can be easily examined while enhancing our understanding in how wetlands are evolving. Topography and elevation are key variables because marsh vegetation is found only within limited elevation gradients identified by specific physical and biological factors, so small alterations in the elevation can change the vegetation pattern within the marsh (e.g., Suchrow & Jensen, 2010; Hladik & Alber, 2012; Buffington et al., 2016; Rogers et al., 2018). For this reason, reliable digital elevation models (DEMs) are essential for estimating marsh areas vulnerable to potential SLR and storm surges (e.g., Hladik & Alber, 2012; Clough et al., 2016; Rogers et al., 2018).

A major objective of the United States Fish and Wildlife Service (USFWS) is to conserve coastal resources by conducting SLR vulnerability assessments for all coastal refuges using the Sea Level Affecting Marshes Model (SLAMM) (USFWS, 2010). DEMs are essential baseline datasets used in SLAMM, so model predictions are prone to the vertical accuracy and errors of interpolated DEMs (Clough et al., 2012). Simulating wetland conversions due to long-term SLR requires low (better) vertical accuracy DEMs. Light Detection and Ranging (LiDAR) have become the standard for building DEMs in coastal environments due to their low vertical accuracy (e.g. <15 cm) and high horizontal resolution (e.g. <5 m). However, it is a challenge for LiDAR to obtain accurate three-dimensional measures in coastal National Wildlife Refuge (NWR) critical habitat areas such as wetlands due to the complexity of coastal marshes.

1.4. LiDAR errors and uncertainties in coastal marshes

The acquisition of accurate elevation measurements in wetlands stems from the instrumentation, software and the complexity of the marsh itself. Many elements, such as data collection, a LiDAR's sensor, the slope of the topography and different filtering techniques, can cause error to occur of the LiDAR data. LiDAR elevation data is shown through x and y (horizontal) and z (vertical) coordinates and the different positions can also contain error through the GNSS, inertial measurement unit (IMU), and/or the laser beam's direction and range (Cooper et al., 2013). Hodgson et al. (2005) concluded that an error in the z coordinate can occur from the land cover type and density depending on the vegetation height and type. According to Hladik and Alber (2012), LiDAR is restricted in its ability to reach the "true" ground in coastal wetland environments from the thick vegetation, even with emerging technological advancements in GNSS, sensors, IMU, and filtering methods, which impacts the accuracy of the LiDAR measurements. Coastal marshes are typically inundated with turbid waters during tidal sequences, have areas of standing water, and often have dense and diverse plants and contain organic soils. All of these items individually make it difficult for the laser to capture the ground surface.

LiDAR point clouds and DEMs often overestimate marsh ground elevations by as much as 0.65 m (Medeiros et al., 2015). This value can vary considerably and the error is often highest in denser and taller the vegetation (Hladik & Alber, 2012). LiDAR is considered to be more accurate the smaller the error of the measurement is, and LiDAR accuracy mainly focuses on the vertical error, which is an important component in SLR vulnerability mapping and assessment of coastal wetlands. Error is a measurement of the difference between an observed value and its actual value and is composed of random and systematic errors (Cooper et al., 2013). Random

errors cause variations around the actual value caused from problems in acquiring measurements, and systematic errors are constant and predictable variations from the actual value from problems in equipment calibration (Johnson, 2018). Systematic errors can come from the sensor, aircraft, GNSS, LiDAR point processing, and geography (Hodgson et al., 2005). Bias, or systematic error approximation, can potentially be managed when the source is determined (Cooper et al., 2013) and can improve LiDAR DEMs.

Without correcting the LiDAR data, elevation cannot truly reveal vegetation, hydrological patterns or the underlying topography, since the distribution of marsh vegetation is linked to the correlation of hydroperiods and elevation (Zhang et al., 2018). Several efforts have been made to address the inability to accurately capture marsh complexity with remote sensing techniques.

One approach is to apply a minimum binning procedure where the minimum LiDAR ground elevation point is assigned to a grid cell when more than one LiDAR point falls within that grid cell (Schmid et al., 2011; Medeiros et al., 2015; Buffington et al., 2016). Minimum binning has also shown to reduce bias and vertical error of LiDAR data collected in heavily vegetated marshes (Schmid et al., 2011; Medeiros et al., 2015; Buffington et al., 2016; Cooper et al., 2019). A second approach is to use Real Time Kinematic (RTK) Global Navigation Satellite Systems (GNSS) to calculate a species-specific bias used to correct the LiDAR DEM. While this simple bias-correction procedure has shown to successfully reduce the bias (Hladik & Alber, 2012; McClure et al., 2016; Cooper et al., 2019), it can be less successful at reducing the vertical error (Rogers et al., 2018; Cooper et al., 2019). This has led researchers to seek a third approach that reduces both bias and error using machine learning techniques (Rogers et al., 2018; Cooper et al., 2019).

The application of machine learning techniques to identify complex and often nonlinear relationships between model predictor variables has proven valuable in correcting LiDAR DEMs of coastal marshes (Rogers et al., 2018; Cooper et al., 2019). While an advantage to machine learning techniques can be a significant reduction in both bias and error, these techniques are more complex and computationally intensive when compared to the minimum binning and bias-correction procedures. However, it is unlikely that an entire vegetation species needs a constant correction using the bias-correction technique (Rogers et al., 2018) because a species presents a range of elevation uncertainty opposed to a constant (Rogers et al., 2016). Therefore, a fourth approach was developed, which combines machine learning with Object-Based Image Analysis (OBIA) techniques that addresses the bias-correction issue where spatial bias is assumed to be homogenous for an entire vegetation community (Cooper et al., 2019). OBIA analyzes and classifies basic segments from images so that segments can be validated, and errors can be removed (Veljanovski et al., 2011). The object-based machine learning (OBML) technique was tested on coastal marsh, swamp, and prairie in the Everglades, and the authors recommend its application in other regions to examine its robustness (Cooper et al., 2019). The application of the OBML approach for LiDAR DEM correction in North Carolina's coastal marshes has potential to enhance the results of SLAMM simulations.

1.5 Sea Level Affecting Marshes Model (SLAMM)

SLAMM is an empirical and mathematical model that is used to show how long-term SLR may potentially impact wetlands and coastlines. SLAMM is attractive because it is open source, has quick computational time, and only a few publicly accessible inputs are required (Wu et al., 2015). Critical inputs that influence the ability of SLAMM to predict landscape alterations include vertical accretion, DEM, rates of sedimentation, and trends in SLR (Chu-Agor et al.,

2011). The model uses a flexible decision tree that produces both tabular and graphical data (NOAA, 2018) and can conduct an uncertainty analysis producing confidence intervals and probability statistics (Clough et al., 2016). Many studies have examined the reliability of SLAMM to predict whether a wetland will survive by migrating inland with increasing SLR. For example, one study compared a bathtub model with SLAMM to find that SLAMM generated the best results for classifying potential habitat change (Zhu et al., 2015). In another study, the ability of LiDAR and RTK-GNSS elevation data to determine the risk of increased inundation using SLAMM was compared, and it was found that RTK-GNSS measurements provided the more reliable simulation results (Murdukhayeva et al., 2013). Incorporating RTK-GNSS measurements into the SLAMM model has potential to help improve our understanding of how North Carolina's coastal marshes may be impacted to future SLR.

1.5.1 SLAMM Limitations

Details provided from the SLAMM simulations are very helpful for understanding and predicting how coastal habitats will change over time from SLR, but there are uncertainties that should be acknowledged. Many landcover models, like SLAMM, are unable to reflect the natural, ecogeomorphic feedbacks that occur in wetland environments which aids in elevation change in response to SLR, and because of this shortcoming SLAMM simulations tend to predict major changes in land cover from increased SLR (Kirwan et al., 2016). Elevation, accretion, and erosion rates are dynamic, which is not taken into account in the SLAMM, so the amount of habitat change may be over/underestimated depending upon the ecogeomorphic feedbacks, like vegetation structure (Wang & Temmerman, 2013; Kirwan et al., 2016). SLAMM considers elements, like accretion and erosion, to be constant over time but the feedback loops cause that not to be the case. Using very coarse land cover data limit's the model's accuracy (Scarborough,

2009) and SLAMM implements the NWI by USFWS, which has a coarse resolution impacting the results. Elevation data accuracy has also shown to restrict SLAMM's capability to predict changes in wetland environments (Wu et al., 2015), making elevation an important baseline parameter to improve and will be focused on in this study.

Another limitation is that SLAMM is not a hydrodynamic model, so it is unable to imitate the water flow rates, which is a major element impacting the dynamics in wetland environments. Hurricanes and storm surges also have the potential to change the topography and sediment dynamics on the coast (Turner et al., 2006; Woods Hole Group, Inc., 2016), which are difficult to capture in SLAMM. Future SLR projections are an additional uncertainty implemented into the model that varies by location but has one of the largest influences on the model. Although, SLAMM comes with limitations it has shown to be a useful tool for coastal managers to use in predicting coastal landcover from SLR.

1.6 Objectives

The main objective of this study is to extend the OBML LiDAR correction approach by Cooper et al. (2019) to a coastal marsh in North Carolina for assessing potential habitat change due to SLR. The specific objectives of this study are as follows: 1) compare the corrected, OBML DEM and the uncorrected, best available LiDAR DEM as critical baseline inputs in SLAMM, 2) compare SLAMM simulations between the corrected, OBML DEM and uncorrected, best available DEM for the year 2050, 3) assess the percentage of potential habitat change due to SLR and produce potential habitat change maps, and 4) gain a better understanding of how North Carolina's coastal marshes may be impacted with future SLR.

2. Study area

The study site is located at Swanquarter National Wildlife Refuge (SNWR) of Hyde County in eastern North Carolina (Figure 1). SNWR is operated as part of the Mattamuskeet, Swanquarter and Cedar Island National Wildlife Refuge Complex. The refuge provides habitat and protection for migratory waterfowl and other birds, along with various other kinds of wildlife. Hunting, fishing and birdwatching are the main reasons people visit the refuge (USFWS, 2018). The study site at SNWR is located off Rose Bay that leads to the Pamlico River and Pamlico Sound. The refuge is a microtidal environment, which are generally more impacted from the effects of SLR. Ocean currents influence the weather, which impacts the type of vegetation and wildlife. On average, the largest amount of rainfall occurs in July and August and the least amount occurs in November and April (Hosier, 2018). SNWR is found in the coastal plain physiographic region and is home to various habitat types, such as irregularly flooded, brackish marsh and forested wetlands. This study focuses on the brackish marsh and the estuarine fringe loblolly pine forest.

The brackish marsh in SNWR is found along the edge of the sound and is generally considered a high marsh since irregularly flooding occurs there mostly from wind tides. The marsh experiences low salinity because the freshwater inflow is greater. Mud flats may occur if the marsh experiences regular flooding combined with the low salinity, which could cause mineral deposition (USFWS, 2008). Overall, this habitat is found on organic peat soils (USFWS, 2018). Black needlerush (*Juncus roemerianus*) is the most prominent vegetation type at SNWR in the brackish marsh but extensive patches of saltmeadow cordgrass (*Spartina patens*), sawgrass (*Cladium jamaicense*), and giant cordgrass (*Spartina cynosuroides*) can also be found. Other vegetation can be found throughout the marsh but is not as extensive (USFWS, 2008). Black

needlerush is generally found at lower elevations of the marsh (area between Mean Low Water (MLW) and Mean High Water (MHW)) (Lynn Haven River Now, n.d.). Eleuterius (1984) found black needlerush to occur at about 0.65 m above MLW. Saltmeadow cordgrass and giant cordgrass are typically found at higher elevations of the marsh (area above MHW) (Lynn Haven River Now, n.d.).

The dominating vegetation for the estuarine fringe loblolly pine forest includes saltmeadow cordgrass, loblolly pine, wax myrtle, and inkberry and is situated on mineral or organic soils (USFWS, 2018). The estuarine fringe loblolly pine forest is found at slightly higher elevations, so it does not flood very often and the loblolly pine is able to grow at sea-level of a coastal plain (Schultz, 1997). Loblolly pine (*Pinus taeda*) provides the overstory and the understory is composed of wax myrtle (*Morella cerifera*) and inkberry (*Ilex glabra*). Saltmeadow cordgrass (*Spartina patens*) mostly covers the floor of the forest (USFWS, 2008). Wax myrtle, inkberry, and loblolly pine are all found at higher elevations than the surrounding wetland and are found in pocosin habitat, which is a wetland that has woody shrub vegetation (NOAA, 2020).

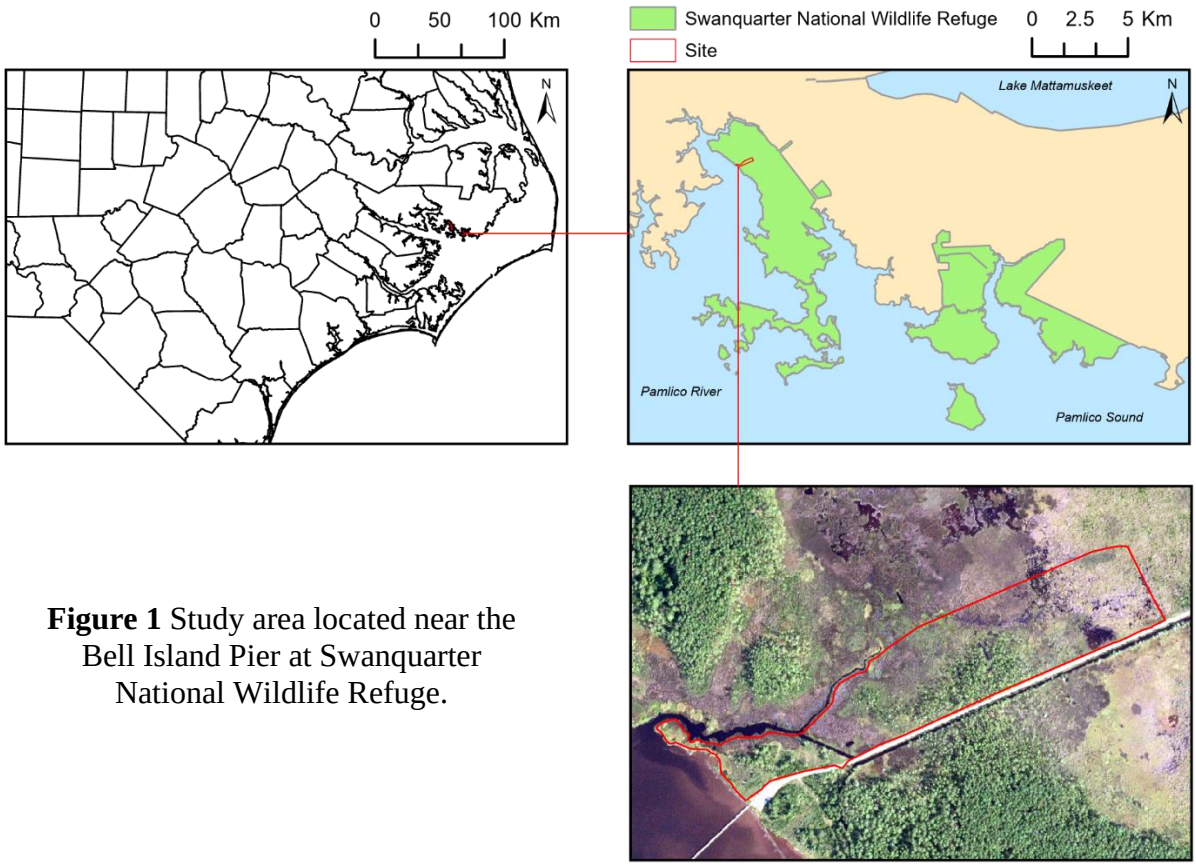

Figure 1 Study area located near the Bell Island Pier at Swanquarter National Wildlife Refuge.

3. Methods

The processing and analysis involved multiple steps and these were outlined as a workflow (Figure 2). An overview of the workflow shows an OBML DEM that was created through image segmentation, LiDAR normalization, data matching, and random forest machine learning. An accuracy assessment was conducted on both the NCFMP DEM and OBML DEM to compute statistics. A SLAMM analysis was run on the NCFMP and OBML DEMs, which required DEMs with VDATUM transformations, slope creations, SLAMM categorized land cover data, and accretion and erosion rates. The initial conditions were calibrated and then simulations were run for the year 2050 for both the NCFMP and OBML DEMs.

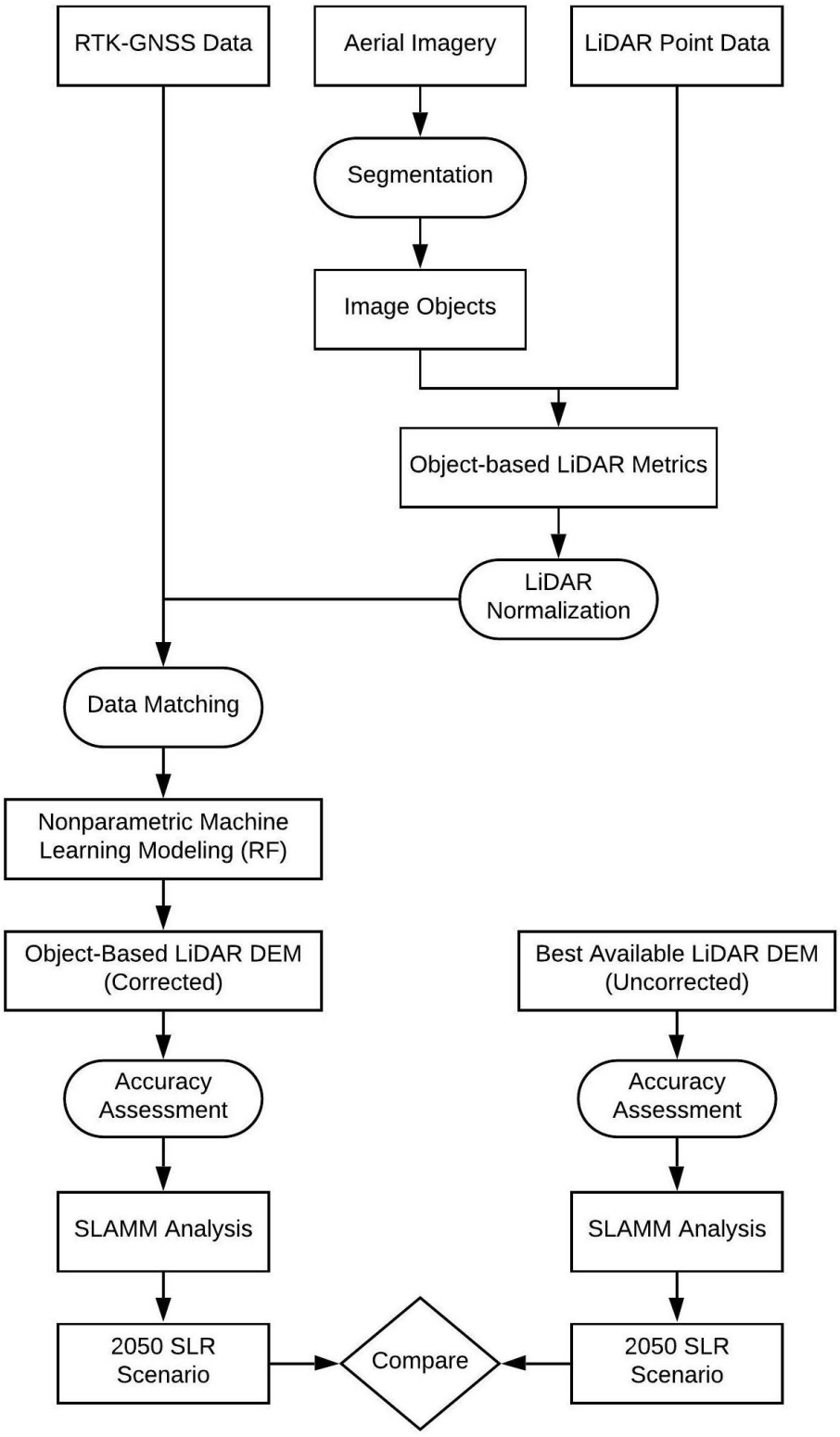

Figure 2 Framework for corrected, OBML DEM approach and the uncorrected, NCFMP DEM approach implemented in SLAMM.

3.1 Data

Data sources used in this study include RTK-GNSS data for correcting the LiDAR point cloud elevations, intensity images from the LiDAR data for normalizing LiDAR point cloud elevations and creating objects, LiDAR point cloud elevations for generating the OBML DEM used in the SLAMM simulation, aerial imagery for generating image objects from OBIA, the National Wetlands Inventory (NWI) dataset to characterize the different land cover types in SLAMM, and the current best available North Carolina Floodplain Mapping Program (NCFMP) DEM for comparison.

RTK-GNSS surveys were conducted for this study in spring 2019 to be seasonally consistent with the LiDAR and aerial imagery. RTK-GNSS locations of the marsh were chosen to help show the subtle changes in elevation by focusing on the different dominant vegetation cover classes. The survey site was accessed off Bell Island Road at SNWR, and care was taken to not disturb the vegetation and sediment as much as possible. Ground control points were collected with Trimble Spectra Precision SP80 RTK-GNSS, which has high-precision static post-processed accuracy of 3 mm in the horizontal and 3.5 mm in the vertical (Root Mean Square Error, RMSE) (Trimble, 2017). The base station was set up at a position for a minimum of 2 hours during each field survey. A topo shoe was equipped on the survey rods of the rovers to avert the instrumentation from sinking into the marsh. The RTK-GNSS rover was positioned level with the marsh surface from 60-180 epochs to record each location. Vegetation type and height was recorded simultaneously with RTK-GNSS locations, and vegetation was grouped dependent upon its height and species. The vegetation height was a measurement of the top vegetation's canopy. A step-point intercept sampling method was used to collect the RTK-GNSS and vegetation locations by taking ten steps perpendicular to Bell Island Road as straight as the

landscape in the marsh would allow, as well as alongside the tidal creeks, creating transects. This method was chosen since it was better for vegetation monitoring because it allowed for a more rapid point collection. However, the step-point method does include sampling bias from maneuvering the difficult wetland landscape. Objects were also created in the field by collecting RTK-GNSS measures around a distinguishable vegetation patch, which would be helpful for verifying object shapes and sizes in eCognition. After collecting the survey data, the receiver's raw files were then automatically adjusted with the National Oceanic Atmospheric Administration's (NOAA) Online Positioning User Service (OPUS) solution using Trimble Business Center v5.10 with an overall RMSE of 0.017 m. The maximum standard deviation for all RTK-GNSS measures combined revealed 0.026 m in the horizontal (0.017+0.009) and 0.032 in the vertical (0.017+0.015).

The current best available LiDAR classified point data for the study site was collected by the United States Geological Survey (USGS) for the NCFMP in Spring 2014 obtained from NOAA data access viewer. The data was developed using North Carolina State Plane Coordinate System, North American Datum of 1983 (NAD83) for the horizontal datum, and North American Vertical Datum of 1988 (NAVD 88) using GEOID12A for the vertical datum. No accuracy assessment was reported in the metadata for the LiDAR classified ground returns; therefore, an accuracy assessment was performed on the ground returns before generating an OBML LiDAR DEM for this study. The NCFMP generated a 1.5 m horizontal resolution hydro-flattened LiDAR DEM from these classified ground returns using interpolation methods. They report a vertical accuracy of 6.3 cm, and the horizontal accuracy of 1 m, both as the RMSE in open terrain. No accuracy assessment was performed for SNWR on the NCFMP DEM. Therefore, an accuracy assessment was performed on the NCFMP and OBML DEM generated in

this study for comparison. The LiDAR classified ground returns and existing NCFMP DEM are available at the National Oceanic and Atmospheric Administration's (NOAA's) data access viewer (https://coast.noaa.gov/dataviewer).

The NWI are used in this study to characterize the different land cover types. The NWI land cover information was derived from imagery collected 1998-2017 and is published by the U.S. Fish and Wildlife Service at: https://www.fws.gov/wetlands/Data/Data-Download.html. The current best available aerial imagery for the study area is the Coastal North Carolina National Agriculture Imagery Program (NAIP) orthophoto imagery with a 1 m horizontal resolution. The imagery was collected spring 2016 using a Leica ADS-100 digital sensor with Red, Green, Blue, and Near-Infrared image bands. The present NAIP horizontal accuracy specifications require 1 m imagery to match within +/- 6 m to true ground specifications. The aerial imagery will be used in this study to generate image objects and is also available for download at NOAA's data access viewer.

3.2 OBML DEM creation

3.2.1 Image Segmentation

A multi-resolution image segmentation method was used to create objects of the different vegetation patches on the study site from aerial imagery in eCognition Developer (Benz et al., 2004; Trimble, 2017), which is known as OBIA. Image segmentation divides images into separate pixel segments, which are then merged with adjacent segments to generate a user-defined heterogeneous threshold (Benz et al., 2004). Color/shape, smoothness/compactness, and scale are important input parameters defined for the algorithm. An optimal scale parameter needs to be determined because a larger scale parameter allows for larger heterogeneous objects, while a smaller scale creates smaller homogeneous objects (Cooper et al., 2019). Zhang et al. (2018)

found a scale of 75 to be most optimal for the marsh classification in that study, but Cooper et al. (2019) found a smaller scale of 30 to work best for wetland elevation mapping. Therefore, different scales were tested in this study ranging from 10 to 75 by aligning the results with the RTK-GNSS points that were collected around different vegetation boundaries. The scale of 10 was found to align best with the RTK-GNSS points along with using a shape parameter of 0.9 and compactness parameter of 0.5. Following the segmentation, elevation statistical measures (mean, minimum, maximum, range, standard deviation) were obtained for every object using the original LiDAR point elevations (Cooper et al., 2019).

3.2.2 LiDAR Normalization

Vegetation height may serve as an important explanatory variable in the OBML modeling for image classification of differing vegetation classes (Onojeghuo & Onojeghuo, 2017). One way to obtain vegetation heights throughout the study area is by LiDAR normalization, which is a method to standardize the LiDAR data. Many normalization procedures were found in the literature where one study extracted the height of a mangrove forest canopy to the mudflat defined by the LiDAR point elevation by using the point height mean, the point height standard deviation, and the point height variation coefficient (Li et al., 2019). In another study, Montealegre et al. (2015) used various interpolation types to normalize LiDAR data to obtain the best, suitable DEM to predict the formation of vegetation in a forested region. Several studies subtracted a DEM from a Digital Surface Model (DSM) to find the correct height (Dash et al., 2004; Brennan & Webster, 2006). For this study, it was apparent the vegetation elevation was being considered the "ground" elevation, so vegetation height was normalized by subtracting a corrected LiDAR DEM from a LiDAR DSM using Esri's ArcMap, which is explained in further detail below.

First, a DEM was generated from the classified LiDAR ground returns using Empirical Bayesian Kriging (EBK), which is a geostatistical interpolation approach that works to create an effective and acceptable kriging model (ESRI, 2016). Through trial and error, an empirical transformation and K-Bessel semivariogram provided the lowest cross-validation results. The NWI land cover raster was used to represent the different vegetation communities, which was resampled to the EBK DEM using so the rasters shared the same cell size of 1 m. The NWI and EBK DEM were then matched with the RTK-GNSS measures where the mean bias between the EBK DEM and RTK-GNSS measures could be calculated for each NWI land cover (Table 1). The EBK was then corrected by the mean bias for each land cover so that the elevation better represented the RTK-GNSS measures.

Table 1 Mean difference or mean bias between the EBK DEM and RTK-GNSS by National Wetland Inventory (NWI) land cover type, all in meters.

NWI Land Cover	Mean Bias = (EBK DEM – RTK-GNSS)
Water	0.36
Unconsolidated Shore	0.38
Palustrine Scrub Shrub Wetland	0.26
Palustrine Forested Wetland	0.19
Palustrine Emergent Wetland	0.52
Impervious Developed	0.69
Estuarine Scrub Shrub	0.43
Estuarine Emergent Wetland	0.51

The next step was to create the DSM from all classified ground returns (i.e., ground and vegetation). With the environment settings configured to the EBK DEM (Geostatistical Analyst), EBK was performed on all classified LiDAR returns using an empirical transformation and K-Bessel semivariogram to create the EBK DSM. Finally, in Raster

Calculator the EBK DEM was subtracted from the EBK DSM creating the normalized vegetation height (Figure 3), which could then be related to the image objects and LiDAR statistical measures.

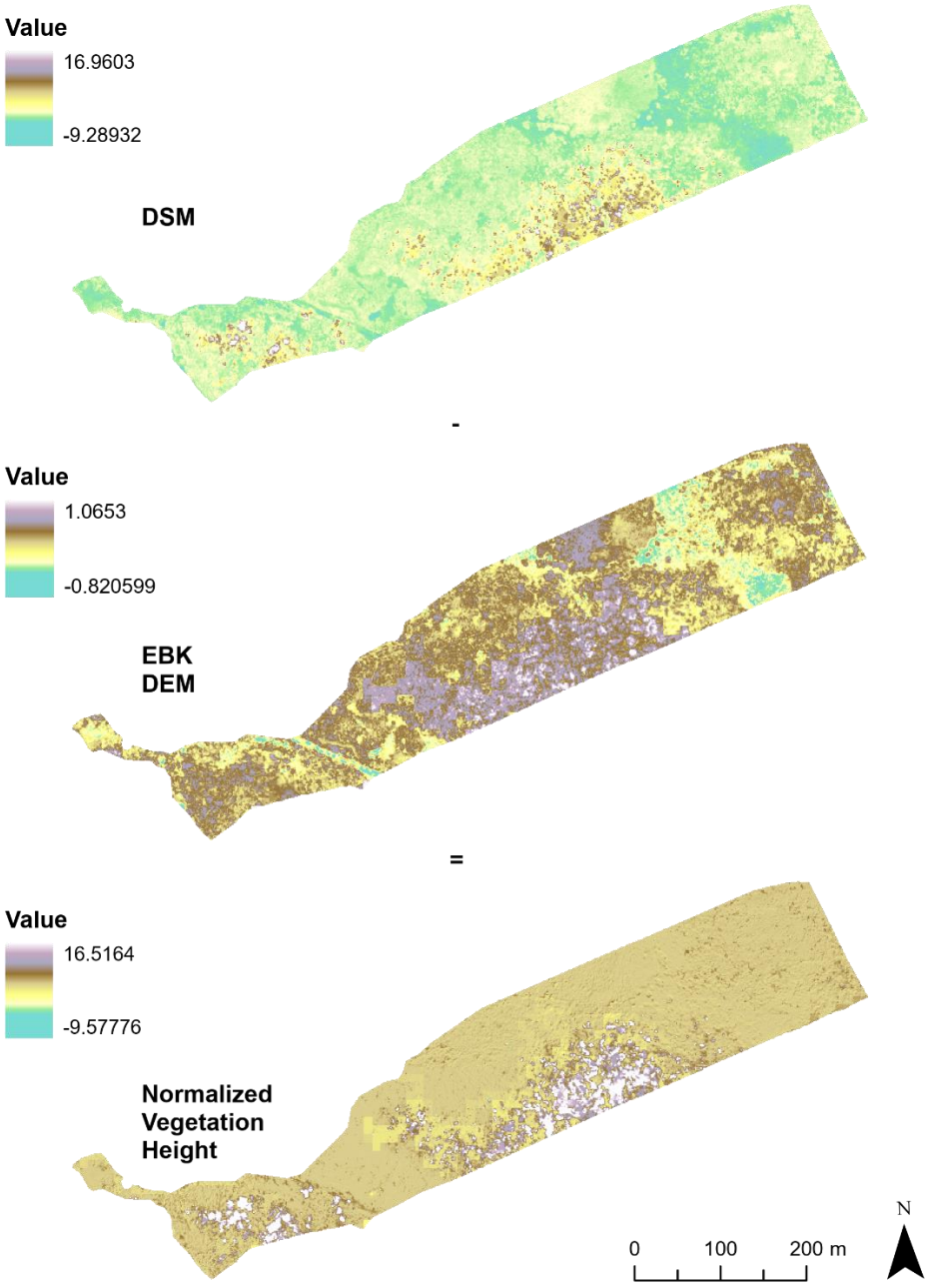

Figure 3 DSM minus EBK DEM equals the normalized vegetation height showing an over/underestimating of the elevation, all in meters.

3.2.3 Data matching

Once the image objects were created and related with LiDAR statistical measures and normalized vegetation height, they were matched with RTK-GNSS. By matching at the object level, the positional uncertainty is reduced between the RTK-GNSS and LiDAR measurements, and vegetation can be better characterized with an object than a grid cell (Cooper et al., 2019). Using OBIA to match the RTK-GNSS to objects is a better option than using a grid because vegetation communities have differing shapes and sizes.

3.2.4 Random Forest machine learning

In this study, a nonparametric machine learning algorithm, Random Forest (RF), was used for ground elevation modeling. RF is an ensemble classifier and regression approach that has a fast processing speed, can handle complicated predictor relationships, and has shown to be useful in mapping the topography of wetland communities (Rogers et al., 2018; Cooper et al., 2019). Breiman (2001) created RF to improve the accuracy of the classification and regression of the decision tree approach. A decision tree classifies the variable with a value that gives the greatest homogeneous groupings of a population. Multiple trees are used in RF and are grown to the largest extent by using different samples and different initial variables to classify a new object. For RF to be conducted, a set number of chosen variables is required so each node can be split in a tree. The matched RTK-GNSS and LiDAR point cloud metrics (mean, minimum, maximum, range, standard deviation) were used, where the RTK-GNSS is the dependent variable and the LiDAR point cloud metrics are the independent variables. But first, the matched samples are randomly split into two datasets; one dataset (Calibration (80%) of 251 points) to guide RF to correct the LiDAR measurements prior to creating a DEM and a second dataset (Validation (20%) of 63 points) to assess RF's final model prediction (shown in Figure 4).

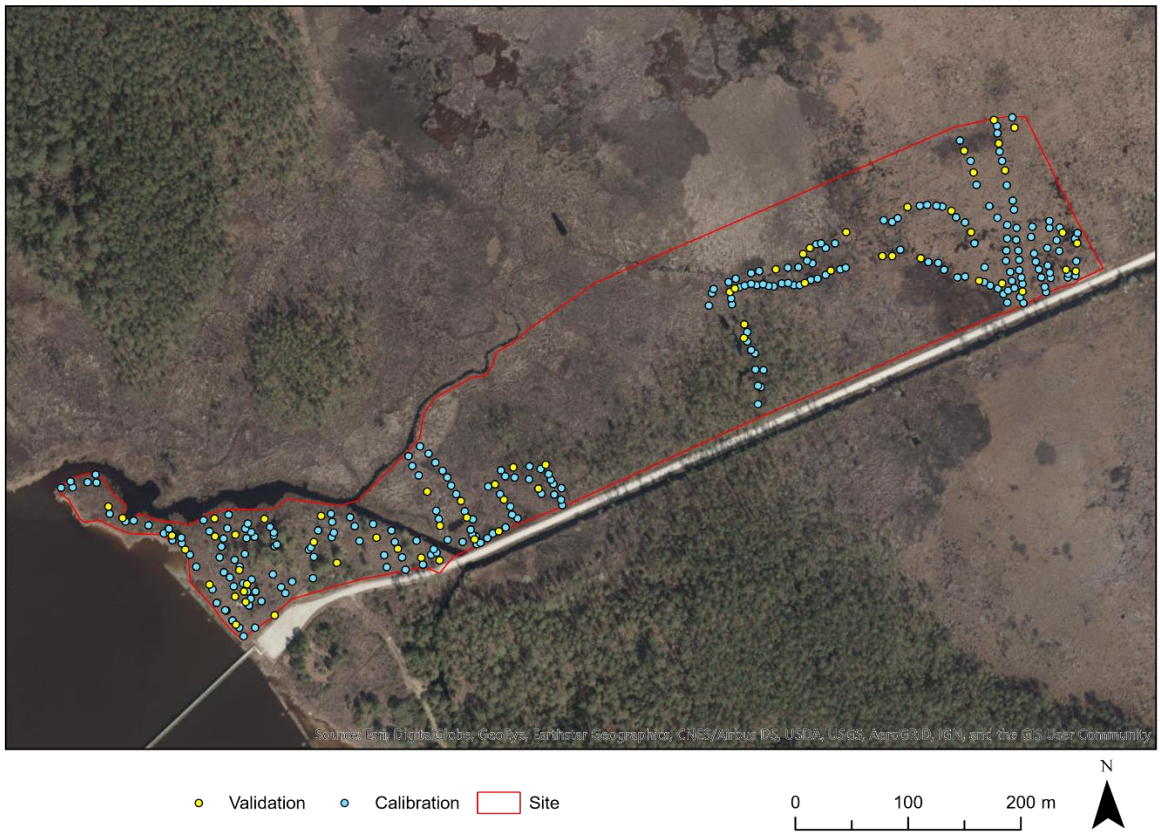

Figure 4 Calibration and Validation GNSS points at study site.

RF was carried out in Waikato Environment for Knowledge Analysis (WEKA, Version 3.8.3), an open source software that performs data mining tasks (Frank et al., 2016, appendix: https://www. cs.waikato.ac.nz/ml/weka/Witten_ et_al_2016_ appendix.pdf). The attribute/feature selection technique identifies the most significant explanatory attribute in a dataset, which can improve the dataset's accuracy and performance, and reduce the amount of training and overfitting (Hall et al., 2009). This technique was used to determine the dependent variables that were used in each RF trial run. RF parameters were adjusted through trial and error, which included specifying the amount of decision trees to create and the amount of subgroup variables randomly chosen from the total variables used for splitting every node in a tree. 100 was used for

the number of decision trees, and the variables that produced the lowest cross-validation RMSE were used, which were the mean of the normalized vegetation height, mean near-infrared (NIR) values, mean brightness values, and minimum LiDAR elevation. Once the RF model calibrated, it was used to make new predictions. The RF prediction results were implemented in Esri's ArcMap creating an OBML DEM by spatially joining predicted attributes to their respective objects (Cooper et al., 2019). Hereinafter, this DEM is referred to as OBML DEM.

3.3 DEM accuracy assessment

R is used in RStudio, which computes statistics, and was used in this study to perform an independent accuracy assessment on the best available NCFMP DEM and OBML DEM generated in this study. In a new R script, the working directory was set, and the "psych" package was installed and loaded from the Comprehensive R Archive Network (CRAN) into RStudio. The "psych" package is a toolbox that offers different functions to calculate descriptive statistics between the validation dataset and the NCFMP and OBML DEMs. The validation .csv files of the two raster files (NCFMP and RF OBIA) were imported into R as a data frame (a table/2-D structure where each column contains values of one variable and each row contains one set of values from each column) using the utils package.

The relationship between the predicted (*P*) (NCFMP and OBML DEMs) and elevation observed measures (*O*) (RTK-GNSS) were analyzed using summary and difference measures. The mean and standard deviation (sd or σ) were the summary measures calculated. The sd displays the range of errors around the mean between the predicted (*P*) and the observed (*O*). The difference measures that were calculated were the Mean Bias Error (MBE) and the RMSE. The MBE, or bias, is any systematic error that causes all the predictions to be off by an amount. MBE is the mean of all the errors/differences between *P* and *O*, and the RMSE is the square root

of the mean squared differences between the *P* and *O*. Results are typically the best when there is a small sd, MBE, and RMSE.

The describe function in the psych package was used to calculate summary statistics for both prediction data frames**,** which produced the variable, count, mean ($\bar{P}$), sd (σ_P), minimum, maximum, range, skew, and kurtosis. The describe function was also used to calculate the elevation observation mean ($\bar{O}$) and standard deviation (σ_O). The difference between the raster elevation-predicted (*P*) and observed (*O*), also called to the error, was calculated and a column was added into the data frame. The MBE was then calculated from the average of all the errors by using the describe function. The RMSE was also calculated (the square root of the mean squared differences between the *P* and *O*).

3.4 SLAMM analysis

The steps that were used to create SLAMM simulations closely followed the SLAMM technical documentation (Warren Pinnacle Consulting, Inc., 2016a) and user guide (Warren Pinnacle Consulting Inc., 2016b). SLAMM analyses were conducted to compare the output using the NCFMP DEM with the output using the OBML DEM for the year 2050.

3.4.1 DEM Transformations and Slope Creations for SLAMM

SLAMM uses the vertical datum of MTL (Mean Tidal Level), thus the NCFMP and OBML DEMs need to be converted accordingly. In this study VDATUM (https://vdatum.noaa.gov), a datum transformation tool from the National Oceanic and Atmospheric Administration (NOAA), was used to convert elevations from NAVD88 to MTL. Since VDATUM does not extend inland much beyond the coast, these areas were transformed vertically using MTL defined by the nearest tide station, which is Beaufort station, NC. MTL at the Beaufort Station is 4 cm below NAVD88, so to bring all inland NAVD88 elevations to MTL,

4 cm was added to the NCFMP and OBML DEMs using the Raster Calculator tool in ArcMap. In addition to DEMs vertically referenced to MTL, SLAMM requires a slope raster for input. Using the OBML DEM, a slope raster was created using ESRI's ArcGIS slope tool (Spatial Analyst). Slope was applied in degrees for each cell to allow a range of elevations for partial cell conversion (Clough et al., 2016).

3.4.2 Land cover data for SLAMM

National Wetland Inventory (NWI) wetland categories that are in vector format need to be changed to SLAMM wetland categories in raster format to run SLAMM simulations. These classifications are found in the SLAMM's technical documentation (http://warrenpinnacle.com/prof/SLAMM6/SLAMM_6.7_Technical_Documentation.pdf). A lookup table was used to assign SLAMM classifications to every NWI polygon using Esri's ArcGIS by adding a new numeric field to the NWI database that contains the appropriate SLAMM classification. The NWI data, classified as SLAMM categories, were transformed to a grid to match the NCFMP and OBML DEMs as well as the slope raster.

3.4.3 Accretion and Erosion Rates for SLAMM

Accretion in a wetland influences its response to SLR. Vertical accretion and sedimentation can counterbalance SLR impacts, which is why it is an important model parameter, along with erosion rates. Horizontal erosion can occur where marshes of SNWR and the open sound meet from the movement of waves, which was observed while conducting fieldwork in this study. Accretion and erosion rates for the different vegetation communities for the study site were included to improve the performance of SLAMM. Accretion rates for high marshes on the east coast were evaluated from various sources and ranged from 0.37 – 0.41 cm/year (Cahoon et al., 1998; Reed et al., 2008; Warren Pinnacle Consulting, Inc., 2012). In one

study, 0.37-0.46 cm was used for black needle rush *Juncus roemerianus* and 0.078-0.111 cm used for saltmeadow cordgrass *Spartina patens* (Cahoon et al., 1998), which are two of the dominant species at the study site. For this study, accretion and erosion rates were used from a previous study at SNWR (Warren Pinnacle Consulting, Inc., 2012), which were 3.7 mm/year for regularly-flooded marsh accretion, 4.1 mm/year for irregularly-flooded marsh accretion, 5.9 mm/year for tidal-fresh marsh accretion, 5.9 mm/year for inland-fresh marsh accretion, 1.1 for tidal swamp accretion, 0.3 mm/year for swamp accretion, 1.8 m/year for marsh erosion, 1 m/year for swamp erosion, and 0.5 m/year for tidal flat erosion. The value for regularly-flooded marsh accretion was from accretion measurements made at Cedar Island NWR (Cahoon et al., 1998), irregularly-flooded marsh accretion was obtained from other U.S. east coast marshes and tidal-fresh marsh and inland-fresh marsh accretion was from regional accretion measurements (Reed et al., 2008). These values were collected through radiometric dating or a Surface Elevation Table). SLAMM defaults were used for tidal swamp and swamp accretion rates and marsh, swamp, and tidal flat erosion rates (Warren Pinnacle Consulting, Inc., 2016a).

3.4.4 SLR Projections for SLAMM

The IPCC is an international administration that reviews and publishes scientific information on climate change. This organization creates SLR projections, which are continually updated with advanced information, modeling, and technologies. The Sea Level Rise and Coastal Flood Hazard Scenarios and Tools Interagency Task Force, established by the National Ocean Council (NOC) and the U.S. Global Change Research Program (USGCRP), monitor and update scenarios of global mean sea level rise (GMSL) determined by the most current, scientific research for coastal planning and management. Probabilistic projections of GMSL are dependent on greenhouse gas emissions and the warming of the earth, whereas relative sea level (RSL)

consists of the change in ocean level and VLM. Sea level does not rise uniformly but spatially variable. One reason for this irregularity is the movement of ocean mass caused by long and short-term variations in air pressure, air to sea heat and freshwater fluxes, ocean currents, and winds. Global sea-levels change from ocean warming and fresh water from ice that melts into the ocean. Local sea-levels change from fluctuations in global sea levels, land elevation changes, ocean circulation and wind patterns (NOAA et al., 2017). Tide gauges measure the rising and falling of the sea, which is different for each coast (NOAA: Ocean Today, n.d.). Along the U.S. east coast, the RSL has shown to be higher than the global average and will continue to increase. Also, the Carolinas are experiencing downward VLM, which in turn increases the RSL on the coast (NOAA et al., 2017).

Many assessment reports have been published by the IPCC, and SLR projections have changed over the years. It is important to be familiar with SLR and the accompanying processes to understand future projections. SLR projections by IPCC are predominately structured by greenhouse gas emissions. One working group within IPCC assesses emission scenarios for possible socio-economic growth throughout the century, resulting in scenarios with differing emission intensities (different energy uses), which have been continually modified throughout the years. Representative Concentration Pathways (RCPs) were created by researchers and have been implemented by the IPCC (Church et al., 2013). Representative denotes to various scenarios that have comparable radiative forcing (energy imbalance before the climate can rebound (Archer, 2012)), concentration is the amount of emissions, and pathways is the long-term trajectories of the greenhouse gas emissions and radiative forcing results (Moss et al., 2008). There are four RCPs (RCP2.6, 4.5, 6, 8.5), each with a differing radiative forcing (2.6, 4.5, 6, 8.5 w/m^2, respectively). RCPs are used in the IPCC assessment reports giving several SLR

projections, and the newest report is the Fifth Assessment Report (AR5, 2013). Ice sheet components are an important addition to AR5 that impacts SLR, however, thermal expansion is predicted to have the largest impact on SLR throughout the century. AR5 uses process-based models creating a GMSL rise range having at least a 66% likelihood of being true to that range (Church et al., 2013), however, this may be deemed inadequate for planners who require a higher percentage of certainty (NOAA et al., 2017). These scenario projections have continued to evolve and advance with updated research and improved technologies and models. Global SLR, as well as fluctuations in local VLM and sea-surface height (SSH), is a major problem for coastal communities and habitats, which is why projecting future SLR is critical for planning purposes.

Long-term SLR causing coastal flooding is an increasing problem for coastal environments. The rise in GMSL will continue to increase and at a faster rate throughout the 21st century producing more intense high tides, storm surges and wave action. This sea level change can begin alterations in ecological systems of wetlands along the coast, which in turn can change the geomorphology of the coast (e.g., sediment buildup), moving where the flood risks may occur for the future (NOAA et al., 2017). Sea level science has been continually advancing over the years and sea level rise, GMSL and RSL, have continued to be revised with new information. To create RSL change projections, processes impacting the SSH and VLM must be accounted for, along with any spatial patterns, which should be at the same degree as the GMSL rise projections (NOAA et al., 2017). Hall et al. (2016) and Kopp et al. (2014) have generated RSL rise estimations based on future GMSL rise estimates. Hall et al. (2016) used the Parris et al. (2012) GMSL rise scenarios to make regional adjustments, while Kopp et al. (2014) created probabilistic projections of GMSL rise scenarios to determine regional adjustments. Both are used to create the most updated science and methodologies to modify GMSL regionally.

The study site will only require local subsidence so relative SLR estimates will be produced, and the SLAMM scenarios will not need adjusting between global (eustatic) and local (relative) SLR trends (Clough et al., 2016). SLR estimates were obtained from the United States Army Corps of Engineers (USACE) sea level rise curve calculator Version 2017.55 (http://corpsmapu.usace.army.mil/rccinfo/slc/slcc_calc.html). This web-based calculator computes projected rates of sea level change to help evaluate the impacts, responses and adaptations required for the present and future. The nearest tide station available for this calculator is at Beaufort, NC. The intermediate scenario was chosen for this study, being a more conservative choice for coastal land managers to use (Figure 5). By the end of the century there is predicted to be at least a meter rise in sea level at Swanquarter National Wildlife Refuge (SNWR). 48 cm was plugged into SLAMM, instead of 47 cm, because mean tidal level (MTL) is 1 cm more than mean sea level (MSL), according to the Beaufort tidal gauge (https://tidesandcurrents.noaa.gov) for the year 2050.

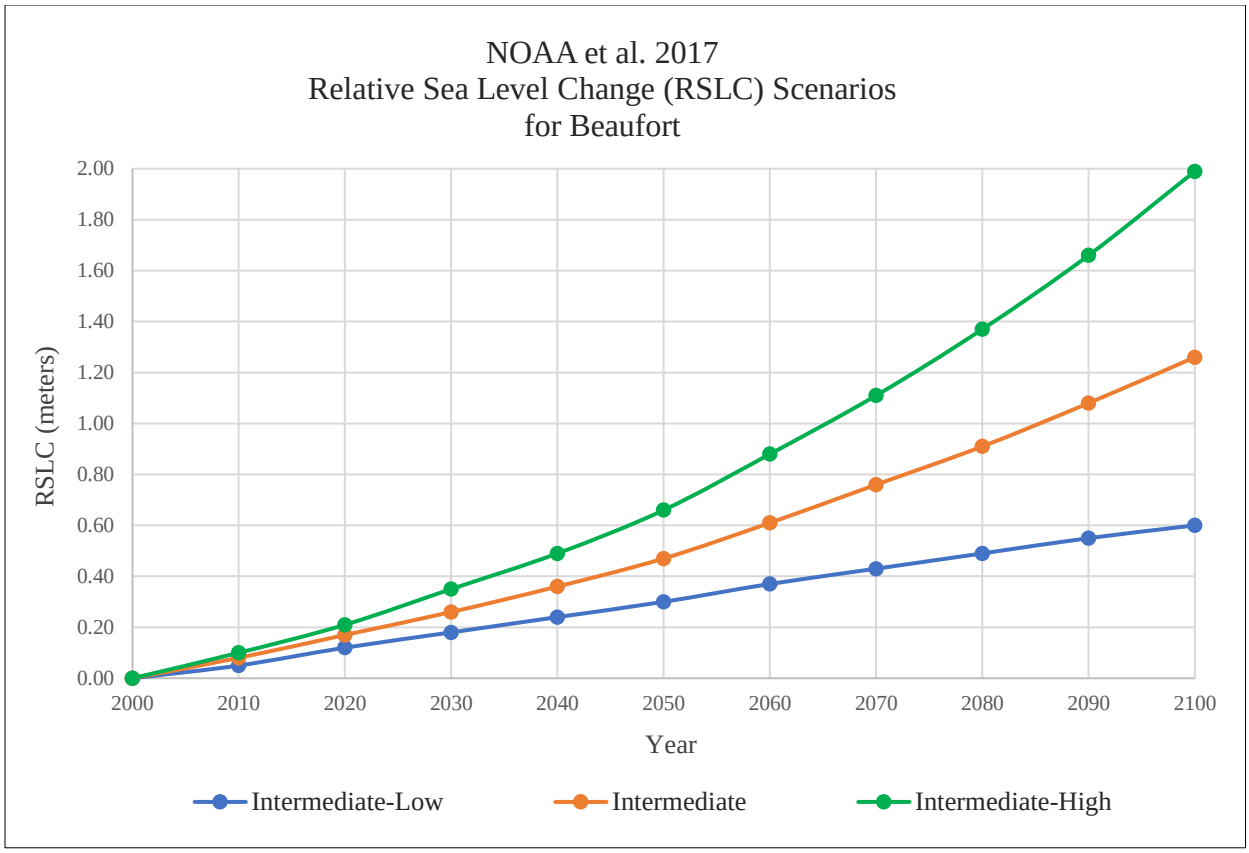

Figure 5 Beaufort, NC sea level-rise projections comparing intermediate-low, intermediate and intermediate high. Data obtained from NOAA et. al (2017) referenced in MSL.

3.4.5 Initial Conditions and Calibration in SLAMM

Before future habitat change modeling can be completed, an initial conditions map of SNWR from SLAMM needs to be calibrated by using a "time-zero" timestep. An initial conditions map was created from a new simulation using general SLAMM categories. The NCFMP and OBML DEMs, NWI converted to SLAMM categories and slope file (in degrees) are the files required for the SLAMM simulation to run. 1998 was the year for the NWI photo date entered (beginning image year of the NWI photo range) and the date of the DEMs was 2014. The south was the direction offshore and the GT Great Tidal Diurnal Tide Range, which is the difference between the Mean Higher-High Water (MHHW) and Mean Lower-Low Water

(MLLW), was 1.079 m, according to the gauge at Beaufort (https://tidesandcurrents.noaa.gov). The MTL minus NAVD88 was kept at 0 because the difference was already calculated into the DEMs. No other site parameters were used to set the initial conditions for this study. The model was run for the specific year of 1998. According to New York State Energy Research and Development Authority (NYSERDA) (2014), having a threshold tolerance up to 5% land cover change in total is considered an appropriate amount for calibration. With SLAMM being calibrated, predicting land cover change for the year 2050 can now be modeled.

3.4.6 2050 SLR Scenarios: NCFMP DEM vs. OBML DEM

The steps for the file setup were repeated from the initial conditions map, but additional site parameters were applied including SLR and accretion to assess the potential impacts of SLR in SNWR by the year 2050. A 3.1 mm/year was used for the historic trend of sea level rise, which is used to approximate the uplift/subsidence, and 1.7 mm/year was used for the historic eustatic trend based on data from the NOAA tide gauge station at Beaufort, NC (https://tidesandcurrents.noaa.gov). The horizontal erosion rates for marsh (1.8 m/year), swamp (1 m/year) and tidal flat (0.5 m/year) were included, as well as the vertical accretion rates for regularly-flooded marsh (3.7 mm/year), irregularly-flooded marsh (4.1 mm/year), tidal-fresh marsh (5.9 mm/year), inland-fresh marsh (5.9 mm/year), tidal swamp (1.1 mm/year), and swamp (0.3 mm/year) (Warren Pinnacle, 2012). The beach sedimentation, which is the vertical accretion for tidal flats and beaches, was also included from that study as 0.5 mm/year. The model was run for the specific year of 2050 with SLR set at 0.48 m after the site parameters had been set.

SLAMM outputs included both tabular and graphic formats. The output maps display predicted habitat divisions and inundated regions based on the different levels and rates of SLR correlated with each scenario.

4. Results

4.1 DEM Results

A large difference can be seen between the two DEMs (Figure 6). When compared to the OBML DEM, the NCFMP DEM clearly overestimates the ground elevation by several meters. Also apparent in the OBML DEM is the grouping of high elevation in two areas (shown in dark orange), which are loblolly pine forest where elevations are much higher than those of the surrounding marsh. This can be confirmed with observations made in the field. The NCFMP DEM may have been interpolated incorrectly causing the areas of higher elevation, where the loblolly pine forest is, to seem to have a lower elevation than the surrounding marsh. The OBML DEM better represents the topography spatially when compared to the NCFMP DEM. Using different DEMs can have major impacts on the results and can change the conclusions of a study.

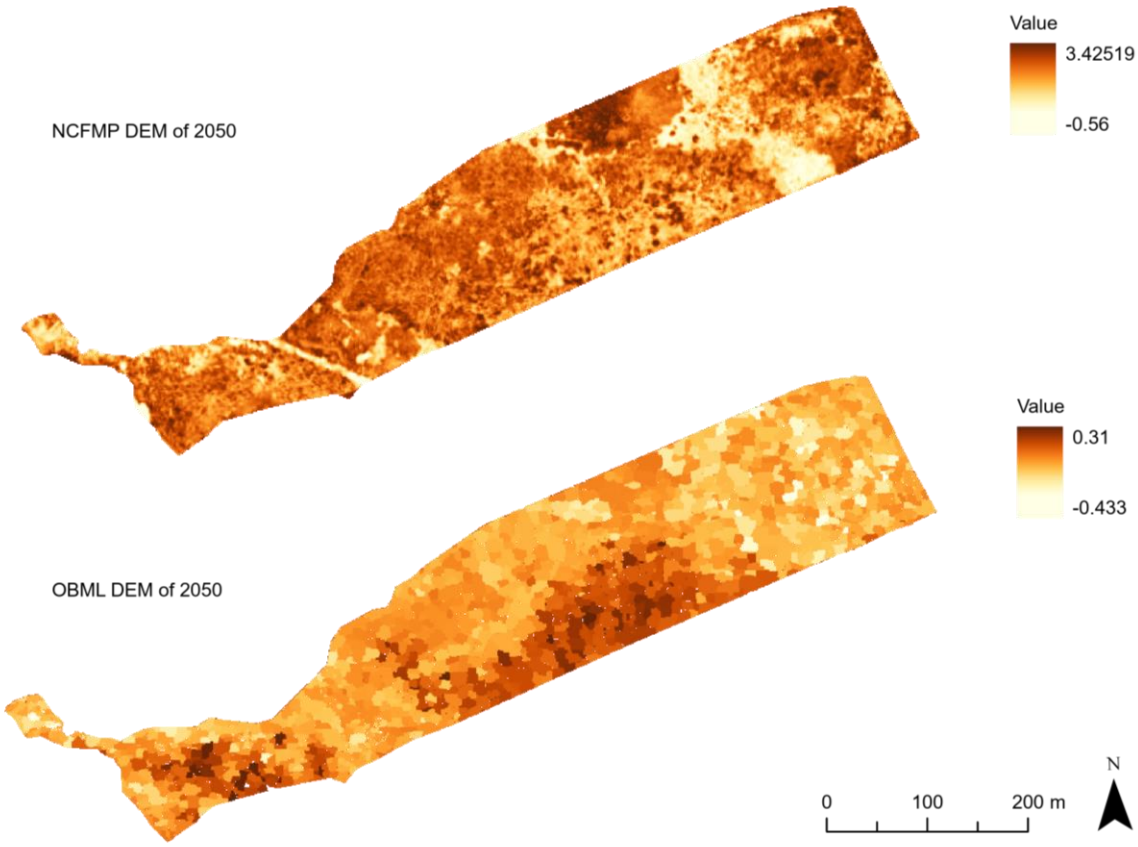

Figure 6 Comparison of the NCFMP DEM with the OBML DEM. Elevations are relative to local Mean Tidal Level (MTL) in meters.

Table 2 Independent accuracy assessment on the NCFMP DEM and OBML DEM created in this study. Where $(\bar{O})$ = the average of elevation observations (RTK-GNSS validation data), $(\bar{P})$= the average of elevation predictions defined by each DEM, (σ_O) and (σ_P) are the standard deviations of the observations and predictions, (σ_{P-O}) is the standard deviation of the differences between the *P* and *O*, MBE = Mean Bias Error, RMSE = Root Mean Square Error, and *n* = number of measures, all in meters (except *n*).

DEM	*n*	$(\bar{O})$	$(\bar{P})$	(σ_O)	(σ_P)	(σ_{P-O})	MBE	MAE	RMSE
NCFMP	63	0.05	1.96	0.1	0.42	0.44	1.91	1.87	1.96
OBML	63	0.05	0.03	0.1	0.06	**0.11**	**-0.01**	**0.06**	**0.11**

When comparing the NCFMP DEM with the OBML DEM, the OBML DEM displays a lower/better MBE, RMSE, and standard deviation (σ) (Table 2). The observed mean ($\bar{O}$) of 0.05 indicated that the average predictions ($\bar{P}$) of the NCFMP DEM (1.96 m) greatly overestimated the corresponding observed parameter $\bar{O}$, while the average predictions ($\bar{P}$) of the OBML DEM (0.03 m) only slightly underestimated the observed mean ($\bar{O}$). The observation data's small standard deviation (σ_O) indicates the data has a tendency to be close to the mean, while a higher standard deviation would have showed a tendency for the data to be more spread out over a broader range of values. The standard deviation of the differences between the *P* and *O* demonstrates that the OBML DEM contains the smallest range of error (σ_{P-O}) of 0.11 m when compared to the NCFMP DEM (σ_{P-O}=0.44 m). Overall, the OBML technique provides an improved DEM of the study area.

4.2 SLAMM Results

4.2.1 SLAMM Calibration

The SLAMM setup and calibration used a threshold of 0.37% land cover change, which is considered appropriate since it is under the threshold tolerance of 5% land cover change (NYSERDA, 2014) (Table 3 and Figure 7). Transitional marsh/Scrub shrub, regularly flooded marsh, and irregularly flooded marsh all decreased, with regularly flooded marsh showing the greatest loss when using a time-step of zero in SLAMM. Only tidal flat showed an increase. No change was seen for the land cover types of inland fresh marsh and estuarine open water.

Table 3 Initial condition of 1998 land cover categories and SLAMM predicted using a "time-zero" time step for calibration.

SLAMM Code	Land Cover	Initial (m^2)	Time Zero (m^2)	Land Cover Change (m^2)	% Change
5	Inland Fresh Marsh	40,318.00	40,318.00	0	0
7	Transitional Marsh / Scrub Shrub	22,226.87	22,225.33	-1.54	0.01
8	Regularly Flooded Marsh	34,266.38	34,155.65	-110.73	0.32
11	Tidal Flat	0	124.22	124.22	0
17	Estuarine Open Water	954.10	954.10	0	0
20	Irregularly Flooded Marsh	23,247.10	23,237.30	-9.80	0.04
				Total	0.37

4.2.2 Initial conditions vs. potential 2050 conditions using NCFMP DEM

The potential change in habitat to the year 2050 was evaluated using the intermediate scenario of 0.48 m MTL from NOAA et al. (2017) for the NCFMP DEM (Table 4). Transitional marsh/scrub shrub and irregularly flooded marsh both showed a loss in habitat, while estuarine open water, regularly flooded marsh and tidal flat show an increase in land cover. No change was seen for inland fresh marsh. Irregularly flooded marsh showed the greatest habitat loss, while regularly flooded marsh showed the greatest habitat increase. Tidal flat was not seen in 1998 but is predicted to occur in SNWR by 2050. From evaluating the maps (Figure 7), areas of irregularly flooded marsh and transitional marsh/scrub shrub are converting to regularly flooded marsh and tidal flat. Also, regularly flooded marsh is converting to estuarine open water on the coastline of the refuge at the marsh-Rose Bay interface. Coastal erosion may be a contributing factor to the increase in estuarine open water, as well as saltwater inundation and increased

frequency and intensity of storm surges. These conversions may reduce species that rely on these environment types to survive.

Table 4 Land cover change by 2050 compared to initial conditions in 1998 using the NCFMP DEM.

SLAMM Code	Land Cover	m^2 in 1998	m^2 in 2050	1998 to 2050 Land Cover Change (m^2)	% Change
5	Inland Fresh Marsh	40,318.00	40,318.00	0	0
7	Transitional Marsh / Scrub Shrub	22,226.87	22,121.72	-105.16	0.47
8	Regularly Flooded Marsh	34,266.38	34,923.33	656.95	1.92
11	Tidal Flat	0	88.86	88.86	*
17	Estuarine Open Water	954.10	1,086.17	132.08	13.84
20	Irregularly Flooded Marsh	23,247.10	22,475.65	-771.45	3.32

4.2.3 Initial conditions vs. potential 2050 conditions using OBML DEM

Table 5 shows the potential change in habitat to the year 2050 using the OBML DEM generated in this study. Inland fresh marsh, transitional marsh/scrub shrub, and irregularly flooded marsh display a loss in habitat, with inland fresh marsh displayed the greatest decrease in habitat, while regularly flooded marsh, tidal flat, and estuarine open water display an increase in habitat. Tidal flat was not seen on the refuge in 1998 but is shown to have the greatest habitat increase by 2050. By evaluating the initial conditions map with the 2050 map derived from the NCFMP DEM and the 2050 map derived from the OBML DEM (Figure 7), many differences can be seen. Marsh migration can be clearly seen from the SLAMM simulation with the OBML DEM. Much of the refuge becomes a tidal flat. Areas that were regularly flooded marsh and transitional marsh/scrub shrub were mostly converted to a tidal flat. Also, inland fresh marsh is mostly converted to regularly flooded marsh and some transitional marsh/scrub shrub. An

increased amount of estuarine open water habitat can be seen along the bay and throughout the area converted into tidal flat. The increased amount of estuarine open water habitat that is seen along the bay is most likely caused by erosion and/or saltwater inundation. The estuarine open water that is seen throughout the area converted into tidal flat could be caused from ponding. Ponding had already started occurring in the refuge already, so it is very reasonable to predict that it will increase in the future with SLR and an increase in storm surges, which are very common in the rivers of the sound.

Table 5 Land cover change by 2050 compared to initial conditions in 1998 using the OBML DEM.

SLAMM Code	Land Cover	m^2 in 1998	m^2 in 2050	1998 to 2050 Land Cover Change (m^2)	% Change
5	Inland Fresh Marsh	40,318.00	0	-40,318.00	100
7	Transitional Marsh / Scrub Shrub	22,226.87	5,089.64	-17,137.24	77.10
8	Regularly Flooded Marsh	34,266.38	34,396.02	129.64	0.38
11	Tidal Flat	0	76,349.30	76,349.30	*
17	Estuarine Open Water	954.10	4,391.99	3,437.89	360.33
20	Irregularly Flooded Marsh	23,247.10	0	-23,247.10	100

4.2.4 Potential 2050 conditions using NCFMP DEM vs. OBML DEM

For 2050, the NCFMP DEM showed no change for inland fresh marsh, while the OBML DEM showed no inland fresh marsh at all. Both DEMs displayed a decrease in transitional marsh/scrub shrub and irregularly flooded marsh. An increase in regularly flooded marsh, tidal flat, and estuarine open water was identified in both DEMs. Overall the NCFMP DEM only showed slight changes in the land cover, whereas the OBML DEM showed major land cover

changes. The NCFMP DEM shows slight marsh migration and the OBML DEM shows a complete restructure of the wetland vegetation (Figure 7).

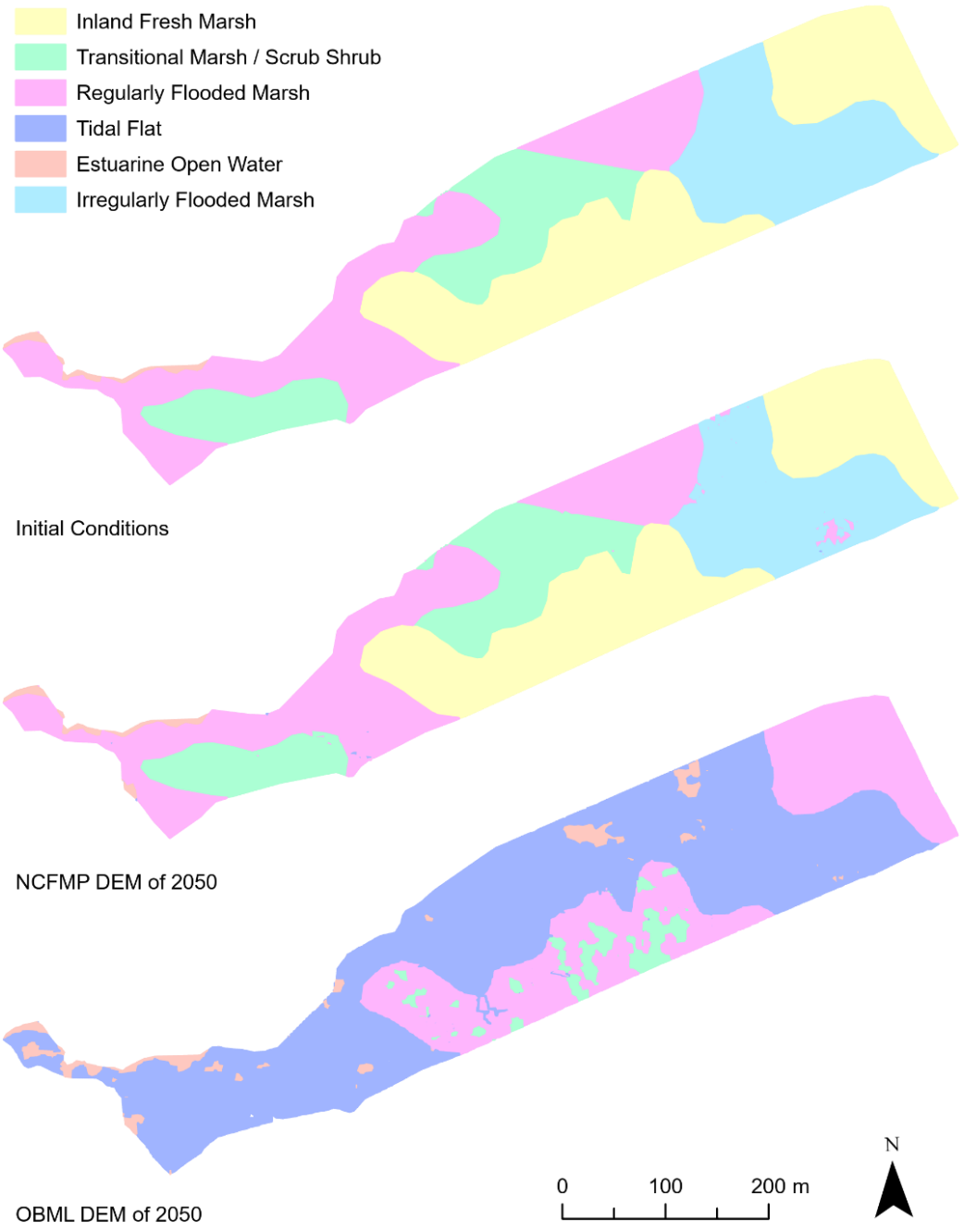

Figure 7 Vegetation cover results for the SLAMM simulations using the intermediate SLR scenario of 0.48 m MTL of the initial conditions of 1998, NCFMP DEM of 2050 and OBML DEM of 2050.

4.2.5 SLAMM Uncertainties

There were uncertainties associated with SLAMM in this study. For example, SLAMM suggests using the USFWS's NWI for land cover data, however, the resolution is very coarse. Implementing a land cover layer that has a better resolution could be beneficial to improve the model's output and thus the results.

The SLAMM simulation for the OBML DEM also showed major land cover changes, but this may be an overestimation since SLAMM does not include the ecogeomorphic feedbacks that take place in wetlands in response to SLR (Kirwan et al., 2016). There are many canals and tidal creeks throughout SNWR, but these hydrodynamic feedbacks are left out of the simulation. Including hydrological factors, like a water depth map, could have the potential to greatly improve SLAMM's predictability since that is not being taken into account and has a major influence. A study at SNWR by Taillie et al. (2019) stated that a vegetation gradient can be seen from brackish marsh to estuarine fringe loblolly pine forest and is reflected with marsh migration and found inundation and salinity tolerance to cause wider transition zone between the forest and marsh vegetation. Salinity in the soil and water was found to have large impact in vegetation patterns, so including this parameter could improve the results of the land cover.

SLAMM results showed an increase in tidal flats for all scenarios but tidal flats are not a common occurrence on the coast of North Carolina. Tidal flats are commonly found in microtidal environments, but with accelerated SLR tidal flats and wetlands generally decrease and wetlands migrate inland. The tidal flat areas may actually be areas that are underwater instead. However, marshes that experience low salinity and regular flooding cause mineral deposition to occur and are known to form tidal flats (USFWS, 2008), so it might be possible for

tidal flats to occur. A critical evaluation of this issue would be helpful for the USFWS in adaptation planning using SLAMM.

5. Conclusion

An OBML technique was utilized in this study to model the potential change in coastal wetland vegetation due to rising sea levels. The objectives of this study were to: 1) examine the potential of the corrected, OBML DEM and the uncorrected, NCFMP DEM as critical baseline inputs in SLAMM, 2) compare SLAMM simulations between the NCFMP and OBML DEMs for the year 2050, 3) assess the percentage of potential habitat change due to SLR and generate corresponding habitat change maps, and 4) gain a better understanding of how North Carolina's coastal marshes may be impacted with future SLR. This research concluded that this method improved elevation modeling and mapping in SLAMM in contrast to using the current best available NCFMP DEM. The following conclusions were found:

- Modeling using an object-based LiDAR correction method, instead of a grid-based method, presents a sounder option for wetland vegetation modeling. Positional inconsistency of an image object and the RTK-GPS metric can be improved with an object-based approach since vegetation is better depicted with an object rather than a grid cell. Using objects helps decrease the bias and uncertainty of a model.
- SLAMM helps provide a representation of the impacts SLR has on coastal habitats. Further environmental dynamics can be evaluated to improve the accuracy of the vegetation community.
- The OBML approach provides a possible representation of the potential impacts of future SLR on coastal wetlands in North Carolina. This approach may become an alternative option for conservation managers to implement for future planning.
- More accurate and precise DEMs can be generated for future research modeling in SLAMM using the object-based LiDAR correction method, and should be used for other

purposes, environmental settings, and in other models to continually improve the method's resilience. Object-based corrected DEMs may improve as new and improved data is collected and more accessible for future research. Possible future research can evaluate the object-based LiDAR correction method in other coastal and wetland models to monitor the changes of vegetation with concern to the elevation and other influencing environmental factors. This method could improve DEMs for generating SLAMM results.

LiDAR DEMs are very important when creating SLR vulnerability assessments, so the accuracy of the DEM is essential. The best available GIS data should be used and improved upon to create a more accurate DEM of a coastal wetland. The OBML approach used in this study has the potential to improve future studies by implementing this technique on other DEMs. Implementing tidal station information when creating a DEM helps improve the DEM for coastal studies and should be included in any future SLR project. SLR projections are also important to include and will improve SLR vulnerability assessments in future research. The OBML approach used in this study should be implemented in other coastal models to increase the robustness of this model. Using this OBML technique on LiDAR DEMs can improve SLR land cover vulnerability assessment mapping practices.

Wetlands are known to be very resilient to changes in SLR, however, this study shows a dramatic change in landcover using only an intermediate SLR scenario, which should be concerning to conservation planners and the surrounding community. Wetlands should be examined at both the regional and global level for the most appropriate coastal planning and protection (Turpie et al., 2015). SLR vulnerability assessments are necessary to be able to monitor and determine adaptation plans for managing coastal wetlands. Although, adaptation

plans conducted by coastal managers of SNWR should be developed with the understanding that there is uncertainty in SLR calculations, which determines wetland migration and differing land cover types will respond differently to SLR in the wetland. The OBML approach to generating DEMs has the potential to improve predictions on SLR impacts for land cover assessments. Additional elements could be included in future studies to improve uncertainties, such as impacts from hurricanes and storm surges, saltwater intrusion, groundwater inundation, etc. SLAMM predictions always have some degree of uncertainty from the uncertainty of the inputs of accretion, elevation, erosion, SLR, subsidence, and tides, which is why creating a study with the most up-to-date and accurate data is needed to produce the best prediction for SLR assessments. It is important for future SLR assessments to include and improve these inputs (wetland feedbacks) to increase the assessments reliability. There are many different elements associated with a wetland system that can and will be impacted as sea-levels continue to rise throughout the century. Each coastal wetland has unique characteristics that differentiates it from other wetlands making their protection to be a very dynamic and complex challenge worldwide. However, it is expected that the OBML approach used in this study will help improve SLR vulnerability assessments to improve adaptation planning measures for coastal wetlands.

References

Archer, D. (2012). *Global Warming: Understanding the Forecast*. (2nd ed.). Chicago, IL: John Wiley & Sons.

Beckett, L.H., Baldwin, A.H., Kearney, M.S. (2016). Tidal Marshes across a Chesapeake Bay Subestuary Are Not Keeping up with Sea-Level Rise. *PLoS ONE, 11*(7), e0159753. doi:10.1371/journal.pone.0159753

Benz, U., Hofmann, P., Willhauck, G., Lingenfelder, I., Heynen, M. (2004). Multi-resolution, object-oriented fuzzy analysis of remote sensing data for GIS-ready information. *Photogrammetry & Remote Sensing, 58*, 239-258.

Bigalbal, A., Rezaie, A.M., Garzon, J.L., Ferreira, C.M. (2018). Potential Impacts of Sea Level Rise and Coarse Scale Marsh Migration on Storm Surge Hydrodynamics and Waves on Coastal Protected Areas in the Chesapeake Bay. *Journal of Marine Science and Engineering, 6*, 86. doi:10.3390/jmse6030086

Breiman, L. (2001). Random Forests. *Machine Learning, 45*, 5-32.

Brennan, R., Webster, T.L. (2006). Object-oriented land cover classification of lidar-derived surfaces. *Can. J. Remote Sensing, 32*(2), 162-172.

Buffington, K.J., Dugger, B.D., Thorne, K.M., Takekawa, J.Y. (2016). Statistical correction of lidar-derived digital elevation models with multispectral airborne imagery in tidal marshes. *Remote Sensing of Environment, 186*, 616 – 625.

Cadol, D., Elmore, A.J., Guinn, S.M., Engelhardt, K.A.M., Sanders, G. (2016). Modeled Tradeoffs between Developed Land Protection and Tidal Habitat Maintenance during Rising Sea Levels. *PLoS ONE, 11*(10), e0164875. doi:10.1371/journal.pone.0164875

Cahoon, D.R., Day, J.W., Reed, D.J., Young, R.S. (1998). Global climate change and sea-level rise: Estimating the potential for submergence of coastal wetlands. *In Vulnerability of coastal wetlands in the Southeastern United States: climate change research results, 1992-97*. U.S. Geological Survey, Biological Resources Division Biological Science Report USGS/BRD/BSR-1998-0002.101 pp. Guntenspergen, G.R., and B.A. Vairin, editors.

Chu-Agor, M., Muñoz-Carpena, R., Kiker, G., Emanuelsson, A., Linkov, I. (2011). Exploring vulnerability of coastal habitats to sea level rise through global sensitivity and uncertainty analyses. *Environmental Modelling & Software, 26*, 593-604.

Church, J.A. & coauthors (2013). Sea level change. Chapter 13 in Climate Change 2013: The Physical Science Basis. Contribution of Working Group I to the Fifth Assessment Report of the Intergovernmental Panel on Climate Change, Cambridge University Press, Cambridge, United Kingdom and New York, NY, USA, 1535.

Clough, J., Park, R., Marco, P., Polaczyk, A., Fuller, R. (2012). SLAMM 6.2 Technical Documentation.

Clough, J., Polaczyk, A., Propato, M. (2016). Modeling the potential effects of sea-level rise on the coast of New York: Integrating mechanistic accretion and stochastic uncertainty. *Environmental Modelling & Software, 84*, 349-362.

Cooper, H.M., Zhang, C., Davis, S.E., Troxler, T.G. (2019). Object-based correction of LiDAR DEMs using RTK-GPS data and machine learning modeling in the coastal Everglades. *Environmental Modelling and Software, 112*, 179-191.

Cooper, H.M., Fletcher, C.H., Chen, Q., Barbee, M.M. (2013). Sea-level rise vulnerability mapping for adaptation decisions using LiDAR DEMs. *Progress in Physical Geography, 37*(6), 745–766.

Dash, J., Steinle, E., Singh, R.P., Bähr, H.P. (2004). Automatic building extraction from laser scanning data: an input tool for disaster management. *Advances in Space Research, 33*, 317-322.

Eleuterius, L.N. (1984). Autecology of the Black Needlerush Juncus roemerianus. *Gulf Research Reports, 7*(4), 339-350. Retrieved from http://aquila.usm.edu/gcr/vol7/iss4/5

Environmental Systems Research Institute, Inc. (ESRI). (2016). What is Empirical Bayesian kriging?. Retrieved from http://desktop.arcgis.com/en/arcmap/10.3/guide-books/extensions/geostatistical-analyst/what-is-empirical-bayesian-kriging-.htm

Frank, E., Hall, M.A., Witten, I.H. (2016). *Data mining: Practical machine learning tools and techniques* (4th ed.). Cambridge, MA: Morgan Kaufmann.

Hall, J.A., Gill, S., Obeysekera, J., Sweet, W., Knuuti, K., Marburger, J. (2016). Regional Sea Level Scenarios for Coastal Risk Management: Managing the Uncertainty of Future Sea Level Change and Extreme Water Levels for Department of Defense Coastal Sites Worldwide. U.S. Department of Defense, Strategic Environmental Research and Development Program. 224 pp.

Hall, M., Frank, E., Holmes, G., Pfahringer, B., Reutemann, P., Witten, I. (2009). The WEKA data mining software: An update. *SIGKDD Explorations, 11*, 10-18.

Hladik, C., Alber, M. (2012). Accuracy assessment and correction of a LiDAR-derived salt marsh digital elevation model. *Remote Sensing of Environment, 121*, 224-235.

Hodgson, M.E., Jenson, J.J., Raber, G., Tullis, J., Davis, B.A., Thompson, G., Schuckman, K. (2005). An evaluation of lidar-derived elevation and terrain slope in leaf-off conditions. *Photogrammetric Engineering and Remote Sensing, 71*(7), 817–823.

Hosier, P.E. (2018). *Seacoast plants of the Carolinas: A new guide for plant identification and use in the coastal landscape.* Chapel Hill, NC: University of North Carolina Press.

Iwamura, T., Possingham, H.P., Chadès, I., Minton, C., Murray, N.J., Rogers, D.I., …, Fuller, R.A. (2013). Migratory connectivity magnifies the consequences of habitat loss from sea-level rise for shorebird populations. *Proceedings of the Royal Society B, 260*(1761). http://doi.org/10.1098/rspb.2013.0325

Johnson, L. (2018). *The Difference Between Systematic & Random Errors*. Sciencing. Retrieved from https://sciencing.com/difference-between-systematic-random-errors-8254711.html

Kirwan, M.L., Temmerman, S., Skeehan, E.E., Guntenspergen, G.R., and Fagherazzi, S. (2016). Overestimation of marsh vulnerability to sea level rise. *Nature Climate Change, 6*, 253-260.

Kopp, R.E., Horton, R.M., Little, C.M., Mitrovica, J.X., Oppenheimer, M., Rasmussen, D.J., Strauss, B., Tebaldi, C. (2014). Probabilistic 21st and 22nd century sea-level projections at a global network of tide-gauge sites. *Earth's Future, 2*(8), 383-406.

Lentz, E.E., Stippa, S.R., Thieler, E.R., Plant, N.G., Gesch, D.B., Horton, R.M. (2015). Evaluating coastal landscape response to sea-level rise in the northeastern United States—Approach and methods (ver. 2.0, December 2015): U.S. Geological Survey Open-File Report 2014–1252, 26 p.

Li, Z., Zan, Q., Yang, Q., Zhu, D., Chen, Y., Yu, S. (2019). Remote Estimation of Mangrove Aboveground Carbon Stock at the Species Level Using a Low-Cost Unmanned Aerial Vehicle System. *Remote Sensing, 11*, 1018.

Linhoss, A.C., Kiker, G., Shirley, M., Frank, K. (2015). Sea-Level Rise, Inundation, and Marsh Migration: Simulating Impacts on Developed Lands and Environmental Systems. *Journal of Coastal Research, 31*(1), 36-46.

Liu, Z., Delach, A. (2015). *Impacts of Sea-Level Rise on National Wildlife Refuges*. Defenders of Wildlife: https://defenders.org/sites/default/files/publications/impacts-of-sea-level-rise-on-refuge-land-protection-priorities.pdf

Lynn Haven River Now. (n.d.). *Tidal wetland plants*. Retrieved from https://norfolk.gov/DocumentCenter/View/28714/LYNN-25637-WetlandsInsrt_Summ15rv-111?bidId=

Maloney, M.C., Preston, B.L. (2014). A geospatial dataset for U.S. hurricane storm surge and sea-level rise vulnerability: Development and case study applications. *Climate Risk Management, 2*, 26–41.

McClure, A., Liu, X., Hines, E., Ferner, M. (2016). Evaluation of error reduction techniques on a LiDAR-derived salt marsh digital elevation. *Journal of Coastal Research, 32*(2), 424-433.

Medeiros, S., Hagen, S., Weishampel, J., Angelo, J. (2015). Adjusting LiDAR-derived digital terrain models in coastal marshes based on estimated aboveground biomass density. *Remote Sensing, 7*, 3507-3525.

Moffett, K.B., Gorelick, S.M. (2016). Alternative stable states of tidal marsh vegetation patterns and channel complexity. *Ecohydrology, 9*, 1639–1662.

Montealegre, A.L., Lamelas, M.T., de la Riva, J. (2015). Interpolation Routines Assessment in ALS-Derived Digital Elevation Models for Forestry Applications. *Remote Sensing, 7*, 8631-8654.

Morris, J.T., Sundberg, K., Hopkinson, C.S. (2013). Salt marsh primary production and its responses to relative sea level and nutrients in estuaries at Plum Island, Massachusetts, and North Inlet, South Carolina, USA. *Oceanography, 26*(3), 78-84.

Moss, R., Babiker, M., Brinkman, S., Calvo, E., Carter, T., Edmonds, J., …, Zurek, M. (2008). *Towards New Scenarios for Analysis of Emissions, Climate Change, Impacts, and Response Strategies*. Intergovernmental Panel on Climate Change, Geneva, 132 pp. Retrieved from Researchgate (No. 236487152).

Murdukhayeva, A., August, P., Bradley, M., Labash, C., Shaw, N. (2013). Assessment of inundation risk from sea level rise and storm surge in northeastern coastal national parks. *Journal of Coastal Research, 29*(6A), 1-16.

National Oceanic and Atmospheric Administration (NOAA). (2020). *What is a pocosin?* National Ocean Service website. Retrieved from https://oceanservice.noaa.gov/facts/pocosin.html

National Oceanic and Atmospheric Administration (NOAA). (2018). Sea Level Affecting Marshes Model. Retrieved February 22, 2019, from https://coast.noaa.gov/digitalcoast/tools/slamm.html

National Oceanic and Atmospheric Administration (NOAA), Sweet W.V., Kopp R.E., Weaver C.P., Obeysekera J., Horton R.M., Thieler E.R., Zervas C. (2017). *Global and Regional Sea Level Rise Scenarios for the United States*. (Report No. NOS CO-OPS 083). Retrieved from https://tidesandcurrents.noaa.gov

National Oceanic and Atmospheric Administration (NOAA): Ocean Today. (n.d.). Global vs. Local Sea Level. Retrieved 4 September 2019 from https://oceantoday.noaa.gov/globalvslocalsealevel/

Neckles, H.A., Lyons, J.E., Guntenspergen, G.R., Shriver, W.G., Adamowicz, S.C. (2015). Use of Structured Decision Making to Identify Monitoring Variables and Management Priorities for Salt Marsh Ecosystems. *Estuaries and Coasts, 38*(4), 1215–1232.

New Hampshire Department of Environmental Services (NHDES). (2004). *Environmental Fact Sheet*. Retrieved from https://www.des.nh.gov/organization/commissioner/pip/factsheets/cp/documents/cp-06.pdf

New York State Energy Research and Development Authority (NYSERDA). (2014). *Applications of Sea-Level Affecting Marshes Model (SLAMM) to Long Island, NY and New York City*. (Report No. 14-29). Retrieved from https://www.ny.gov

Onojeghuo, A.O., Onojeghuo, A.R. (2017). Object-based habitat mapping using very high spatial resolution multispectral and hyperspectral imagery with LiDAR data. *International Journal of Applied Earth Observation and Geoinformation, 59*, 79-91.

Parris, A., Bromirski, P., Burkett, V., Cayan, D., Culver, M., Hall, J., …, Weiss, J. (2012). Global Sea Level Rise Scenarios for the US National Climate Assessment. NOAA Tech Memo OAR CPO-1. 37 pp.

Reece, J.S., Noss, R.F. (2014). Prioritizing Species by Conservation Value and Vulnerability: A New Index Applied to Species Threatened by Sea-Level Rise and Other Risks in Florida. *Natural Areas Journal, 34*(1), 31-45.

Reed, D.J., Bishara, D.A., Cahoon, D.R., Donnelly, J., Kearney, M., Kolker, A.S., …, Stevenson, J.C. (2008). Site-Specific Scenarios for Wetlands Accretion as Sea Level Rises in the Mid-Atlantic Region. Section 2.1 in: Background Documents Supporting Climate Change Science Program Synthesis and Assessment Product 4.1, J.G. Titus and E.M. Strange (eds.). EPA 430R07004. U.S. EPA, Washington, DC.

Rodríguez, J.F., Saco, P.M., Sandi, S., Saintilan, N., Riccardi, G. (2017). Potential increase in coastal wetland vulnerability to sea-level rise suggested by considering hydrodynamic attenuation effects. *Nature Communications, 8*(1), 16094. DOI: 10.1038/ncomms16094

Rogers, J.N., Parrish, C.D., Ward, L.G., Burdick, D.M. (2018). Improving salt marsh digital elevation model accuracy with full-waveform lidar and nonparametric predictive modeling. *Estuarine, Coastal and Shelf Science, 202*, 193-211.

Rogers, J.N., Parrish, C.E., Ward, L.G., Burdick, D.M. (2016). Assessment of elevation uncertainty in saltmarsh environments using discrete-return and full waveform LiDAR. *Journal of Coastal Research*, 76, 107–122 Special Issue.

Scarborough, R.W. (2009). Application of the Sea Level Rise Affecting Marsh Model (SLAMM) Using High Resolution Data At Prime Hook National Wildlife Refuge. Retrieved http://www.dnrec.delaware.gov/coastal/Documents/PHNWR%20SLAMM.pdf

Schile, L.M., Callaway, J.C., Morris, J.T., Stralberg, D., Parker, V.T., Kelly, M. (2014). Modeling Tidal Marsh Distribution with Sea-Level Rise: Evaluating the Role of Vegetation, Sediment, and Upland Habitat in Marsh Resiliency. *PLoS ONE 9*(2): e88760. doi:10.1371/journal.pone.0088760

Schmid, K.A., Hadley, B.C., Wijekoon, N. (2011). Vertical accuracy and use of topographic LiDAR data in coastal marshes. *Journal of Coastal Research, 27*, 116–132.

Schultz, R.P. (1997). *Loblolly Pine: The Ecology and Culture of the Loblolly Pine (Pinus Taeda L.)*. U.S. Forest Service. Retrieved from https://www.srs.fs.usda.gov/pubs/misc/ah_713.pdf

Suchrow, S., Jensen, K. (2010). Plant Species Responses to an Elevational Gradient in German North Sea Salt Marshes. *Wetlands, 30,* 735-746.

Tabak, N.M., Laba, M., Spector, S. (2016). Simulating the Effects of Sea Level Rise on the Resilience and Migration of Tidal Wetlands along the Hudson River. *PLoS ONE, 11*(4), e0152437. doi:10.1371/journal.pone.0152437

Taillie, P.J., Moorman, C.E., Poulter, B., Ardón, M., Emanuel, R.E. (2019). Decadal-Scale Vegetation Change Driven by Salinity at Leading Edge of Rising Sea Level. *Ecosystems, 22*, 1918–1930.

Trimble. (2017). SP80 GNSS Receiver. Available online at: http://trl.trimble.com/docushare/dsweb/Get/Document-844535/SG-SP80-Br-v2.pdf

Turner, R.E., Baustian, J. J., Swenson, E.M., Spicer, J.S. (2006). Wetland sedimentation from hurricanes Katrina and Rita. *Science 314*, 449–452.

Turpie, K.R., Klemas, V.V., Byrd, K., Kelly, M., Jo, Y. (2015). Prospective HyspIRI global observations of tidal wetlands. *Remote Sensing of Environment, 167*, 206-217.

U.S. Army Corps of Engineers (USACE). (2017). Sea-Level Change Curve Calculator. Retrieved from http://corpsmapu.usace.army.mil/rccinfo/slc/slcc_calc.html

U.S. Fish & Wildlife Service (USFWS). (2018). National Wildlife Refuge System: Swanquarter National Wildlife Refuge, North Carolina. Retrieved from https://www.fws.gov/refuge/swanquarter/

U.S. Fish and Wildlife Service (USFWS). (2010). Rising to the urgent challenge: Strategic plan for responding to accelerating climate change. Retrieved from https://www.fws.gov/home/climatechange/pdf/ccstrategicplan.pdf

U.S. Fish and Wildlife Service (USFWS). (2008). Swanquarter National Wildlife Refuge Comprehensive Conservation Plan. Retrieved from https://www.fws.gov/southeast/planning/PDFdocuments/Swanquarter%20Final/Swanquarter%20Final%20CCP%20edited.pdf

Veljanovski, T., Kanjir, U., Oštir, K. (2011). Object-based image analysis of remote sensing data. *Geodetski Vestnik, 55*(4), 641-664.

Veloz, S.D., Nur, N., Salas, L., Jongsomjit, D., Wood, J., Stralberg, D., Ballard G. (2013). Modeling climate change impacts on tidal marsh birds: Restoration and conservation planning in the face of uncertainty. *Ecosphere 4*(4), 49.

Wang, C., Temmerman, S. (2013). Does biogeomorphic feedback lead to abrupt shifts between alternative landscape states?: An empirical study on intertidal flats and marshes. *J. Geophys. Res. Earth Surf., 118*, 229–240.

Warren Pinnacle Consulting, Inc. (2012). Application of the Sea-Level Affecting Marshes Model (SLAMM 6) to Swanquarter NWR. Retrieved from http://warrenpinnacle.com/prof/SLAMM/USFWS/SLAMM_Swanquarter_NWR.pdf

Warren Pinnacle Consulting, Inc. (2016a). SLAMM 6.7 Technical Documentation: Sea Level Affecting Marshes Model, Version 6.7 beta. Retrieved from http://warrenpinnacle.com/prof/SLAMM6/SLAMM_6.7_Technical_Documentation.pdf

Warren Pinnacle Consulting, Inc. (2016b). SLAMM 6.7 beta, User's Manual. Retrieved from http://warrenpinnacle.com/prof/SLAMM6/SLAMM_6.7_Users_Manual.pdf

Woods Hole Group, Inc. (2016). Modeling the Effects of Sea-Level Rise on Coastal Wetlands. Retrieved from https://www.mass.gov/files/documents/2018/12/07/czm-slamm-report-nov2016.pdf

Wu, W., Yeager, K., Peterson, M., Fulford, R. (2015). Neutral models as a way to evaluate the Sea Level Affecting Marshes Model (SLAMM). *Ecological Modelling, 303*, 55-69.

Zhang C., Denka S., Mishra D. (2018). Mapping freshwater marsh species in the wetlands of Lake Okeechobee using very high-resolution aerial photography and LiDAR data. *International Journal of Remote Sensing, 39*(17), 5600-5618.

Zhu, M., Hoctor, T., Volk, M., Frank, K., Linhoss, A. (2015). The conservation value of elevation data accuracy and model sophistication in reserve design under sea-level rise. *Ecology and Evolution, 5*(19), 4376-4388.